

Dear Prof Joos

Once more, we would like to thank you and the referees for their efforts in reviewing our manuscript and providing us with the opportunity to further improve it. We have provided a brief response to the second referee's remaining comments below, and hope that the changes we have made in response to these suggestions meet with your approval. We include a copy of the manuscript with track changes enabled to allow you to more quickly identify where we have made modification to the text.

Yours sincerely,
Yit Arn Teh

RESPONSE TO REFEREE 2

1. Thank you so much to the authors for taking all the reviewers' suggestion to heart. I do like the manuscript, and the improvement are satisfactory. This is a very important manuscript, where the work neatly combines field measurements and laboratory experiments to tease out drivers of nitrous oxide emissions. A few comments remain, but they probably more reflect my ignorance, and elsewhere are more of editorial nature.

AUTHOR RESPONSE: Our sincerest thanks for these kind remarks. We hope the responses we have provided below will be to the referee's satisfaction.

2. Abstract: I am not sure whether unweighted means need to be part of the abstract, as the weighting really more reflect the montane tropical N₂O emissions.

AUTHOR RESPONSE: Because our area- and seasonally-weighted annual flux estimates were conducted as part of a post-hoc exercise, and may contain errors associated with calculations of the areal fractions or may have errors associated with our simple method of temporal weighting, we believe it may be more prudent to indicate both unweighted and weighted annual flux estimates in the abstract. We have since updated the current abstract to include both unweighted and weighted flux estimates (see L35-L41).

3. Abstract L35: Can it be added that this conclusion stems from 15N enrichment experiment?

AUTHOR RESPONSE: We apologise if we have misunderstood the referee, but the data reported in L35 refer to field fluxes. The 15N-nitrate addition experiment did verify that premontane forest showed significantly higher 15N-N₂O production potential than montane grassland and upper montane forest mineral layer soil (see L682-L688), but we were not referring to these data here.

4. Abstract L 53: I suggest to start the last sentence with “Yet, nitrous oxide flux...” to highlight the contrast to the finding of N₂O emission being a function of N richness.

AUTHOR RESPONSE: Editorial suggestion taken.

5. L98 suggest to use “large” instead of “long”

AUTHOR RESPONSE: Editorial suggestion taken. We have also corrected the title (L3) and other parts of the text (L23) to remain internally consistent.

6. L115 This seems at odds with the data, for most of the time WFPS is < 60%

AUTHOR RESPONSE: We must apologise for the lack of precision in our language. Here we were referring to our preliminary dataset, where there were a large proportion of values that were near to or above the 60 % WFPS threshold. The referee is correct that in the longer-term dataset presented in this manuscript, WFPS was generally lower than this threshold, which suggests that the preliminary data were collected during a year that was slightly wetter than the overall average for the whole study period. We have now revised the text to make it clearer that what we are referring to here is our preliminary dataset (L129-L130).

7. Paragraph starting with L 121: In my previous review I suggested to try to work with lags. The authors countered that the time series is too short for doing that. While I am not sure that 30 months is long enough for lag analysis, the visual lag correlation is striking. At the same time, it is probably not the reviewer’s choice on how the analysis should be conducted.

AUTHOR RESPONSE: The referee is correct that there do appear to be lags in the data, but we were unable to pick this out with the statistical analyses that we used. We suspect that these lags may have been obscured by the large variance in the field data, making it difficult to identify statistically significant trends.

8. L233: Check throughout the manuscript to use consistently use “litter-fall” or “litterfall”.

AUTHOR RESPONSE: Editorial suggestion. We have corrected the manuscript so that we use the word “litter-fall” consistently throughout the text. The word “litterfall” was only used once, whereas we “litter-fall” was used in all other instances throughout the text, so we thought it more consistent to use the former form of the word.

9. L241: Not clear what “at the bottom” means when you give a depth range.

AUTHOR RESPONSE: We have now changed the phrase to “deployed in the plant rooting zone” to make the sentence more economical.

10. L261: Can you indicate the N concentration (eg. ug/L), of the isotope solution added?

AUTHOR RESPONSE: The N concentration of the 30 atom % ¹⁵N tracer varied depending on the habitat (Table 2), so we chose to keep the explanation simpler in this part of the text so as not to make the methods more difficult to read. We would prefer to keep the text as it is, for the sake of simplicity of explanation.

11. Result section: I really appreciate the extra work the authors put in to make this section much more readable.

AUTHOR RESPONSE: Thank you for this comment. We really valued this referee’s comments and those of the other referees on the Results, because their suggestion have improved the readability of the text.

12. L 817: Does this contradict L 800, where you say that N poor habitats have a greater proportional response (where you suggest that there is a response to NO₃ addition)?

AUTHOR RESPONSE: Thank you for this comment. One again, the referee has highlighted where we should have been more precise with our language. The text has been revised to better-represent what we were trying to express (L833-L851). In this part of the text, we were trying to explain why we may not have observed an immediate response of the soil microbial community to enhanced NO₃- availability.

13. Figure 3: replace “broken line” with “dashed line”

AUTHOR RESPONSE: Editorial suggestion taken.

1 **1. Title page:**

2

3 **Complex controls on nitrous oxide flux across a large elevation gradient in the tropical**
4 **Peruvian Andes**

Deleted: long elevation

5

6 Torsten Diem^{1,2}, Nicholas J. Morley¹, Adan Julian Ccahuana³, Lidia Priscila Huaraca Quispe³,
7 Elizabeth M. Baggs⁴, Patrick Meir^{5,6}, Mark I.A. Richards¹, Pete Smith¹, and Yit Arn Teh^{1,2*}

8

9 ¹ School of Biological Sciences, University of Aberdeen, UK

10 ² Formerly at the School of Geography and Geosciences, University of St Andrews, UK

11 ³ Universidad Nacional de San Antonio Abad del Cusco, Peru

12 ⁴ The Royal (Dick) School of Veterinary Studies, University of Edinburgh

13 ⁵ School of GeoSciences, University of Edinburgh, UK

14 ⁶ Research School of Biology, Australian National University, Canberra, Australia

15

16 * Corresponding author; yateh@abdn.ac.uk

18 **2. Abstract**

19 Current bottom-up process models suggest that montane tropical ecosystems are weak
20 atmospheric sources of N₂O, although recent empirical studies from the southern Peruvian
21 Andes have challenged this idea. Here we report N₂O flux from combined field and
22 laboratory experiments that investigated the process-based controls on N₂O flux from
23 montane ecosystems across a large elevation gradient (600-3700 m a.s.l.) in the southern
24 Peruvian Andes. Nitrous oxide flux and environmental variables were quantified in four
25 major habitats (premontane forest, lower montane forest, upper montane forest and
26 montane grassland) at monthly intervals over a 30-month period from January 2011 to June
27 2013. The role of soil moisture content in regulating N₂O flux was investigated through a
28 manipulative, laboratory-based ¹⁵N-tracer experiment. The role of substrate availability
29 (labile organic matter, NO₃⁻) in regulating N₂O flux was examined through a field-based litter-
30 fall manipulation experiment and a laboratory-based ¹⁵N-NO₃⁻ addition study, respectively.
31 Ecosystems in this region were net atmospheric sources of N₂O, with an unweighted mean
32 flux of 0.27 ± 0.07 mg N-N₂O m⁻² d⁻¹. Weighted extrapolations, which accounted for
33 differences in land surface area among habitats and variations in flux between seasons,
34 predicted a mean annual flux of 1.27 ± 0.33 kg N₂O-N ha⁻¹ year⁻¹. Nitrous oxide flux was
35 greatest from premontane forest, with an unweighted mean flux of 0.75 ± 0.18 mg N-N₂O m⁻²
36 d⁻¹, translating to a weighted annual flux of 0.66 ± 0.16 kg N₂O-N ha⁻¹ year⁻¹. In contrast,
37 N₂O flux was significantly lower in other habitats. The unweighted mean fluxes for lower
38 montane forest, montane grasslands, and upper montane forest were 0.46 ± 0.24 mg N-N₂O
39 m⁻² d⁻¹, 0.07 ± 0.08 mg N-N₂O m⁻² d⁻¹, and 0.04 ± 0.07 mg N-N₂O m⁻² d⁻¹, respectively. This
40 corresponds to weighted annual fluxes of 0.52 ± 0.27 kg N₂O-N ha⁻¹ year⁻¹, 0.05 ± 0.06 kg
41 N₂O-N ha⁻¹ year⁻¹, and 0.04 ± 0.07 kg N₂O-N ha⁻¹ year⁻¹, respectively. Nitrous oxide flux
42 showed weak seasonal variation across the region; only lower montane forest showed
43 significantly higher N₂O flux during the dry season compared to wet season. Manipulation of
44 soil moisture content in the laboratory indicated that N₂O flux was significantly influenced by
45 changes in water-filled pore space (WFPS). The relationship between N₂O flux and WFPS was
46 complex and non-linear, diverging from theoretical predictions of how WFPS relates to N₂O
47 flux. Nitrification made a negligible contribution to N₂O flux, irrespective of soil moisture
48 content, indicating that nitrate reduction was the dominant source of N₂O. Analysis of the
49 pooled data indicated that N₂O flux was greatest at 90 and 50 % WFPS, and lowest at 70 and

Deleted: long elevation

Deleted: which emitted

Deleted: .

Deleted: ,

Deleted: with

Deleted: emitting

Deleted: montane grasslands emitting

Deleted: upper montane forest emitting

Formatted: Not Superscript/ Subscript

58 30 % WFPS. This trend in N₂O flux suggests a complex relationship between WFPS and
59 nitrate-reducing processes (i.e. denitrification, dissimilatory nitrate reduction to
60 ammonium). Changes in labile organic matter inputs, through the manipulation of leaf litter-
61 fall, did not alter N₂O flux. Comprehensive analysis of field and laboratory data
62 demonstrated that variations in NO₃⁻ availability strongly constrained N₂O flux. Habitat – a
63 proxy for NO₃⁻ availability under field conditions – was the best predictor for N₂O flux, with
64 N-rich habitats (premontane forest, lower montane forest) showing significantly higher N₂O
65 flux than N-poor habitats (upper montane forest, montane grassland). ~~Yet, N₂O~~ flux did not
66 respond to short-term changes in NO₃⁻ concentration.

Deleted: Nitrous oxide

Formatted: Subscript

67
68

69 3. Introduction

70 The tropics are the largest source of atmospheric nitrous oxide (N₂O), accounting for at least
71 half of all global N₂O emissions (Hirsch et al., 2006;Huang et al., 2008;Kort et al.,
72 2011;Nevison et al., 2007;Saikawa et al., 2014). The bulk of tropical N₂O emissions come
73 from terrestrial sources, with the largest emissions arising from agricultural land and
74 unmanaged lowland tropical forests (Hirsch et al., 2006;Huang et al., 2008;Kort et al.,
75 2011;Nevison et al., 2007;Saikawa et al., 2014). However, while we have a relatively robust
76 understanding of the global atmospheric budget as a whole (Hirsch et al., 2006;Huang et al.,
77 2008;Saikawa et al., 2014), our knowledge of regional atmospheric budgets, particularly at
78 the sub-continental scale, is much more limited, due to the constraints imposed by the
79 spatial distribution of existing atmospheric sampling networks and ground-based,
80 ecosystem-scale sampling efforts (Kort et al., 2011;Nevison et al., 2004;Nevison et al.,
81 2007;Saikawa et al., 2014).

82

83 In order to predict and model N₂O flux at these smaller (sub-continental) spatial scales,
84 bottom-up emissions inventories or process-based models are often used, with emissions
85 estimates constrained by empirical measurements (Werner et al., 2007;Li et al., 2000;Potter
86 et al., 1996;Saikawa et al., 2013). However, these models are only as reliable as the data
87 used to parameterize them; as a consequence, ecosystems that are under-represented in
88 the empirical literature or which are poorly understood may be modelled less accurately,
89 with knock-on effects for larger-scale emissions estimates (Saikawa et al., 2013;Teh et al.,

91 2014;Werner et al., 2007). Nitrous oxide dynamics in montane tropical ecosystems are
92 particularly poorly understood, because past research has concentrated on N₂O flux from
93 lowland *tierra firme* forests (Saikawa et al., 2013;Teh et al., 2014;Werner et al., 2007).
94 Montane ecosystems, however, are important components of many tropical landscapes, and
95 account for a sizeable land area. For example, in continental South America, montane
96 ecosystems (>500 m a.s.l.) cover more than 8 % of the land surface (Eva et al., 2004), and
97 play key roles in regional carbon (C), nitrogen (N), and greenhouse gas (GHG) dynamics
98 (Girardin et al., 2010;Moser et al., 2011;Teh et al., 2014;Wolf et al., 2012;Wolf et al., 2011).
99 Process-based models predict that N₂O flux from these montane environments are lower
100 than those from the lowland tropics (i.e. <1.0 kg N₂O-N ha⁻¹ yr⁻¹) (Saikawa et al.,
101 2013;Werner et al., 2007). However, these models have rarely been tested against empirical
102 data, and several field studies indicate that N₂O flux from montane ecosystems can exceed
103 these prior models' estimates (Corre et al., 2010;Teh et al., 2014;Veldkamp et al., 2008). In
104 some instances, N₂O flux from montane ecosystems can in fact approach emissions from
105 lowland forests, begging the question as to whether or not existing models do, in fact,
106 accurately represent flux from these high elevation ecosystems (Corre et al., 2010;Teh et al.,
107 2014;Veldkamp et al., 2008).

108

109 In order to improve our wider understanding of the dynamics and biogeochemistry of N₂O in
110 montane tropical forests, we conducted a combined field and laboratory study to investigate
111 the environmental controls on denitrification and N₂O flux across a large elevation gradient
112 (600-3700 m a.s.l.) in the tropical Peruvian Andes. Prior work from this region indicated that
113 montane ecosystems in this area were stronger sources of N₂O than predicted by bottom-up
114 process models (Teh et al., 2014). In particular, lower elevation premontane and lower
115 montane forests, which account for the majority of the land area in this region (~54 %),
116 showed emission rates that are on par with lowland tropical forests, suggesting that these
117 ecosystems could be important contributors to regional atmospheric budgets (Teh et al.,
118 2014). Nitrous oxide flux appeared to be derived from nitrate reduction (i.e. denitrification,
119 dissimilatory nitrate reduction to ammonium), and was linked to seasonal variations in
120 climate, with N₂O emissions increasing during the dry season compared to the wet season
121 (Teh et al., 2014). However, contrary to theoretical expectations (Davidson, 1991;Firestone
122 and Davidson, 1989;Groffman et al., 2009;Davidson and Verchot, 2000), N₂O flux was not

Deleted: long

124 directly correlated with soil moisture content in our field dataset (Teh et al., 2014), raising
125 unresolved questions about the role of seasonal variations in soil moisture content in driving
126 N₂O flux. We hypothesized that the weak relationship between N₂O flux and soil moisture
127 content was because soil water-filled pore space (WFPS) – an index of soil moisture and a
128 proxy for soil anaerobiosis – normally fell above the theoretical threshold where N₂O flux
129 was constrained by the availability of anaerobic microsites (i.e. ~60 % WFPS) [in our](#)
130 [preliminary dataset](#) (Davidson, 1991; Firestone and Davidson, 1989; Groffman et al.,
131 2009; Davidson and Verchot, 2000; Teh et al., 2014). Even during the dry season, WFPS rarely
132 fell below this threshold value (Teh et al., 2014), allowing other driving variables, such as
133 nitrate (NO₃⁻), to play a more dominant role in regulating N₂O flux (Teh et al., 2014).

134

135 In the work presented here, we extended our time series to multi-annual time scales, in
136 order to better understand the role of longer-term climatic variability in modulating N₂O
137 flux. We also conducted a series of manipulative field and laboratory experiments to
138 investigate the mechanistic controls on N₂O flux in greater detail, and to test hypotheses
139 raised by our earlier work (as described below) (Teh et al., 2014). Furthermore, these
140 manipulative experiments were crucial in helping us interpret our time series of field
141 observations, because prior research indicated that the relationship between individual
142 control variables (e.g. WFPS or NO₃⁻) and N₂O flux were confounded by the simultaneous
143 action of multiple control variables (Teh et al., 2014). The overarching goals of this research
144 were to: investigate how climate and environmental variables regulate N₂O flux over multi-
145 annual time scales; clarify the role of soil moisture as a proximate or distal control on N₂O
146 flux; and evaluate the role of key substrates for nitrate reduction (i.e. labile organic matter,
147 NO₃⁻) in driving N₂O flux. Specifically, we hypothesized that:

148 **H1.** Enhanced N₂O flux during the dry season (i.e. during periods of reduced soil
149 moisture) is due to an increase in N₂O flux from nitrification and reduced N₂O
150 reduction during denitrification

151 **H2.** N₂O flux is poorly correlated with soil water-filled pore space *in situ* because soil
152 moisture content does not normally constrain denitrification under field conditions;
153 however, N₂O flux is closely correlated with water-filled pore space when soil
154 moisture content is more limiting for denitrification (i.e. <60 % WFPS)

155 **H3.** N₂O flux increases proportionately with the availability of substrates for
156 denitrification (i.e. NO₃⁻, labile organic matter)
157 In order to address these three objectives and their attendant hypotheses, we quantified
158 N₂O flux and environmental variables from four major habitat types (premontane forest,
159 lower montane forest, upper montane forest and montane grassland) at monthly intervals
160 over a 30-month period. We also conducted manipulative laboratory experiments that
161 investigated how variations in soil moisture content (WFPS) and NO₃⁻ availability influenced
162 N₂O flux. In addition, we manipulated labile organic matter availability through a field-based
163 litter-fall manipulation study, recognizing that labile organic matter plays an important role
164 in supplying not only the reducing equivalents for nitrate reduction, but also indirectly
165 providing inorganic N for ammonia oxidation and nitrate reduction via N mineralization
166 (Morley and Baggs, 2010; Blackmer and Bremner, 1978; Davidson, 1991; Firestone et al.,
167 1980; Weier et al., 1993).

Deleted: litterfall

168
169

170 **4. Materials and methods**

171 **4.1 Study site**

172 Measurements were conducted on the eastern slope of the Andes in the Kosñipata Valley,
173 Manu National Park, Peru (Figure 1) (Malhi et al., 2010). This 3.02 x 10⁶ ha (30,200 km²)
174 region has been the subject of intensive ecological, biogeochemical and climatological
175 studies since 2003 by the Andes Biodiversity and Ecosystem Research Group (or, ABERG;
176 <http://www.andesconservation.org>), and contains a series of long-term permanent plots
177 across a 200-3700 m above sea level (m a.s.l.) elevation gradient that stretches from the
178 western Amazon to the Andes (Malhi et al., 2010). This part of the Andes experiences
179 pronounced seasonality in rainfall but not in air temperature; the dry season extends from
180 May to September and the wet season from October to April (Girardin et al., 2010). Thirteen
181 sampling plots (approximately 20 x 20 m each) were established at four different habitats
182 across a gradient spanning 600-3700 m a.s.l., including premontane forest (600 – 1200 m
183 a.s.l.; n = 3 plots), lower montane forest (1200 – 2200 m a.s.l.; n = 3 plots), upper montane
184 forest (2200 – 3200 m a.s.l.; n = 3 plots), and montane grasslands (3200 – 3700 m a.s.l.; n = 4
185 plots; colloquially referred to as “puna”) (Figure 1). In premontane forest, sampling plots
186 were established in Hacienda Villa Carmen, a 3,065 ha biological reserve operated by the

188 Amazon Conservation Association (ACA), containing a mixture of old-growth forest,
189 secondary forest and agricultural plots (Teh et al., 2014). Sampling for soil gas flux was
190 concentrated in the old-growth portions of the reserve. For lower montane and upper
191 montane forests, sampling plots were established adjacent to or within existing 1 ha
192 permanent sampling plots established by ABERG (Teh et al., 2014). Sampling plots were also
193 established in montane grasslands (Teh et al., 2014). To capture a representative range of
194 environmental conditions, mesotope-scale (100 m-1 km scale landforms) topographic
195 features were sampled (Belyea and Baird, 2006). Mesotopic features include ridges, slopes,
196 flats and a high elevation basin. The latter two landforms include wet, grassy lawns with no
197 discernible grade, and a peat-filled depression, respectively. Summary site descriptions are
198 provided in Table 1. Data on soil properties were collected as part of this study, while mean
199 annual precipitation is from earlier research by ABERG (Girardin et al., 2010).

200

201 **4.2 Soil-atmosphere exchange**

202 Field sampling was performed over a 30-month period from January 2011 to June 2013 for
203 all habitats except for premontane forest. Due to circumstances outside our control, only 24-
204 months of data were collected for premontane forest, with sampling commencing in July
205 2011. Soil-atmosphere flux was collected monthly, except where flooding or landslides
206 prevented safe access by investigators to the study sites. Gas exchange rates were
207 determined with five replicate gas flux chambers deployed in each of the thirteen plots (n =
208 65 flux observations per month). All representative landforms were sampled in each habitat
209 (Table 1).

210

211 Soil-atmosphere flux of CH₄, N₂O and CO₂ were determined using a static flux chamber
212 approach (Livingston and Hutchinson, 1995), although only N₂O flux is reported here.
213 Methane and CO₂ flux are discussed in detail in another publication (Jones et al., 2016).
214 Static flux chamber measurements were made by enclosing a 0.03 m² area with cylindrical,
215 opaque (i.e. dark), two-component (i.e. base and lid) vented chambers with a ~8 L volume.
216 Chamber bases were permanently installed to a depth of approximately 5 cm and inserted
217 >1 month prior to the commencement of sampling, in order to minimize potential artefacts
218 from root mortality following base emplacement (Varner et al., 2003). Chamber lids were
219 fitted with small computer case fans to promote even mixing in the chamber headspace

220 (Pumpanen et al., 2004). Headspace samples were collected from each flux chamber over a
221 30-minute enclosure period, with samples collected at 4 discrete intervals, 7.5 minutes
222 apart, using a gastight syringe. Gas samples were stored in evacuated Exetainers® (Labco
223 Ltd., Lampeter, UK), shipped to the UK by courier, and subsequently analysed for CH₄, N₂O
224 and CO₂ concentrations with a Thermo TRACE GC Ultra (Thermo Fisher Scientific Inc.,
225 Waltham, Massachusetts, USA) at the University of St Andrews. Chromatographic separation
226 was achieved using a Porapak-Q column, and analyte concentrations quantified using a
227 flame ionization detector (FID) for CH₄, electron capture detector (ECD) for N₂O, and
228 methanizer-FID for CO₂. Instrumental precision was determined by repeated analysis of
229 standards and was better than 5 % for all detectors. Gas flux rates were determined using
230 the R HMR package to plot best-fit lines to the data for headspace concentration against
231 time for individual flux chambers (Pedersen et al., 2010; Team, 2012). Gas mixing ratios
232 (ppm) were converted to areal flux by using the Ideal Gas Law to solve for the quantity of gas
233 in the headspace (on a mole or mass basis), normalized by the surface area of each static
234 flux chamber (Livingston and Hutchinson, 1995). Measurements resulting in zero net flux
235 were included in our dataset.

236

237 **4.3 Environmental variables**

238 To investigate the effects of environmental variables on trace gas dynamics, we determined
239 soil moisture, soil oxygen content in the 0-10 cm depth, soil temperature, and air
240 temperature at the time of flux sampling. Volumetric soil moisture content was determined
241 using portable soil moisture probes (ML2x ThetaProbe, Delta-T Device Ltd., Cambridge, UK)
242 inserted into the substrate immediately adjacent to each flux chamber (<5 cm from each
243 chamber base; depth of 0-10 cm). Soil moisture content is reported here as water-filled pore
244 space (WFPS), and is calculated using the measurements of volumetric water content and
245 bulk density (Breuer et al., 2000). Soil O₂ concentration was determined using the approach
246 described by Teh et al. (2014). Soil temperature (0-10 cm depth), chamber temperature and
247 air temperature was determined using type K thermocouples (Omega Engineering Ltd.,
248 Manchester, UK). Data on aboveground litter-fall, meteorological variables (i.e.
249 photosynthetically active radiation, air temperature, relative humidity, rainfall, wind speed,
250 wind direction), continuous plot-level soil moisture (10 and 30 cm depths) and soil

251 temperature (0, 10, 20 and 30 cm depths) measurements were also collected, but are not
252 reported in this publication.

253

254 Resin-extractable inorganic N flux (i.e. ammonium, NH_4^+ ; nitrate, NO_3^-) were quantified in all
255 plots using a resin bag approach (Templer et al., 2005; Subler et al., 1995). From August 2011
256 onwards, ion exchange resin bags (n = 15 resin bags per elevation) were deployed in the
257 plant rooting zone (i.e. 0-10 cm depth in premontane forest, lower montane forest and
258 montane grasslands; 0-15 cm in upper montane forest), following established protocols
259 (Templer et al., 2005; Subler et al., 1995). Samples were collected at monthly intervals
260 (where possible) for determination of monthly, time-averaged NH_4^+ and NO_3^- flux (Subler et
261 al., 1995). For some plots, this sampling frequency was periodically disrupted due to natural
262 hazards (i.e. landslides, river flooding) preventing safe access to the study sites. Resin bags
263 were shipped to the University of Aberdeen after collection from the field, inorganic N was
264 extracted using 2 M KCl and concentrations determined colourimetrically using a Burkard
265 SFA2 continuous-flow analyser (Burkard Scientific Ltd., Uxbridge, UK) (Templer et al.,
266 2005; Subler et al., 1995).

267

268 4.4 Water-filled pore space manipulation study

269 We investigated the effects of WFPS on N_2O flux derived from nitrate reduction or
270 nitrification rates using a ^{15}N tracer experiment. Soil cores for all habitats were collected
271 from the 0-10 cm depth, and were not fully air-dried nor sieved prior to incubation. Soils
272 were distributed into glass jars and adjusted to 10% below the target WFPS values of 30%,
273 50%, 70% and 90%, either by letting the soils partially air-dry or by adding water to them,
274 depending on the WFPS of the soils at the time of collection (n = 5 for each ^{15}N addition and
275 3 controls for each WFPS for a total of n = 212; see Table 2). Additional de-ionized water,
276 containing the ^{15}N tracers, was subsequently added gravimetrically to raise WFPS to target
277 levels. The exception to this was for the upper montane forest, where samples were
278 collected from the 0-10 cm depth of the mineral soil, but not from the organic layer. The
279 reason for this is that the mineral soil layer in the upper montane forest is overlain by a thick
280 organic horizon up to 17 cm deep, consisting of poorly decomposed leaves, roots, and humic
281 materials; very akin to low density peat (Zimmermann et al., 2012; Zimmermann et al.,
282 2009a; Zimmermann et al., 2009b). In contrast, the organic matter in the upper 10 cm soil

Deleted: at the bottom of

284 layer in the other habitats is closely intermixed with the mineral phase, and does not
285 normally constitute a distinct mineral-free horizon. Thus, to sample mineral soil in the upper
286 montane forest, we had to sample beneath this thick organic horizon.

287

288 Two different types of ^{15}N -tracers (30 atom %) were applied to the soils in order to
289 determine the proportion of N_2O derived from nitrate reduction and nitrification (Bateman
290 and Baggs, 2005). $^{14}\text{N-NH}_4^{15}\text{N-NO}_3$ was used to quantify the amount of N_2O produced by
291 nitrate reduction, while $^{15}\text{N-NH}_4^{15}\text{N-NO}_3$ was used to quantify the amount of N_2O produced
292 from both nitrate reduction and nitrification. The difference between the two was used to
293 calculate the amount of N_2O derived from nitrification alone. After application of the tracers,
294 the jars were sealed, and gas samples taken at 0, 6, 12, 24, 36 and 48 hours to determine
295 rates of gas flux. Nitrous oxide yield was calculated as the ratio of $^{15}\text{N-N}_2\text{O}$ flux : $^{15}\text{N-N}_2\text{O}$ flux
296 + $^{15}\text{N-N}_2$ flux. Soils were sampled at the end of the experiment for NO_3^- concentration,
297 NH_4^+ concentraion, and total C and N content.

298

299 Soil gas concentrations (N_2O , CO_2 and CH_4) were measured on a GC as described in section
300 4.2, while $^{15}\text{N-N}_2$ and $^{15}\text{N-N}_2\text{O}$ were measured on a SerCon 20:20 isotope ratio mass
301 spectrometer equipped with an ANCA TGII pre-concentration module (SerCon Ltd., UK). The
302 coefficient of variation (CV; an index of instrumental precision) for repeated analysis of gas
303 concentration and isotope standards was <5 %. $^{15}\text{N-N}_2\text{O}$ and $^{15}\text{N-N}_2$ fluxes were calculated
304 from the ^{15}N atom percent excess of the samples compared to the controls using the HMR
305 package (Pedersen et al., 2010).

306

307 **4.5 Litter-fall manipulation experiments**

308 We conducted a field-based litter-fall manipulation experiment to test for the effects of
309 variations in labile organic matter availability on trace gas flux. This study took place over a
310 14-month period (April 2012 to June 2013), and consisted of 4 experimental treatments
311 (control, +50 % litter addition, +100 % litter addition, litter removal) implemented across 3
312 habitats (premontane forest, lower montane forest, upper montane forest), with 6 replicate
313 plots per treatment per habitat (each treatment plot was 0.5 x 0.5 m in size; n = 24
314 observations per habitat; n = 72 observations per sampling increment). Leaf litter addition
315 rates for the +50 % and +100 % litter addition treatments were determined based on prior

316 research from this study site, and fell within the natural range of variability observed across
317 this elevational gradient (Girardin et al., 2010).

318

319 Litter-fall for the litter addition treatments was collected monthly in litter baskets (n = 3
320 litter baskets per treatment plot for a total of n = 18 per habitat). These data were also used
321 to determine the background rates of leaf litter-fall among habitats. For the control, litter
322 inputs simply reflected natural background litter-fall rates. For the +50 % and +100 % litter
323 addition treatments, background litter inputs were supplemented with additional litter
324 taken from the litter baskets. Briefly, wet litter was weighed in the field using portable scale,
325 gently mixed (homogenized), and then re-distributed to the +50 % and +100 % litter addition
326 plots in amounts proportional to the average amount of wet litter that fell into the litter
327 baskets over the course of the month. As a consequence, the amount of litter added in the
328 two litter addition treatments was not fixed but varied according to the natural background
329 rate of litter-fall. For the litter removal treatment, leaf litter was removed from the forest
330 floor at the start of the experiment, and 3mm nylon mesh was placed over the surface of the
331 treatment plot to prevent further litter ingress to the soil surface. Any debris accumulating
332 on the mesh was removed at monthly intervals.

333

334 Trace gas flux and environmental variables were determined at 7 time points over the
335 course of the 14-month experiment using the methods described in section 4.2. In addition,
336 soil moisture (WFPS from the 0-10 cm depth), soil temperature (0-10 cm depth), air
337 temperature, soil gas concentrations (O₂, CH₄, N₂O, CO₂) from the 0-10 cm and 20-30 cm
338 depths, litter C, and litter N were determined concomitantly. Litter C and N content was
339 determined on a Carlo-Erba NA 2500 elemental analyser (CE Instruments Ltd, Wigan, UK) at
340 the University of Aberdeen.

341

342 **4.6 Nitrate addition experiment**

343 To quantify the effect of NO₃⁻ availability on N₂O flux, we conducted a ¹⁵N-NO₃⁻ addition
344 experiment. Background concentrations of NO₃⁻ were determined prior to the start of
345 experiment using soil subsamples (n = 5 per elevation), after which the soils from each
346 habitat were divided into three treatment groups, and supplemented with surplus NO₃⁻
347 which raised these background levels by +50 %, +100 %, and +150 % (Table 2). The NO₃⁻

348 added to the soil in each of the treatments was enriched with ^{15}N in order to trace the
349 conversion of nitrate to gaseous N products ($^{15}\text{N-N}_2\text{O}$, $^{15}\text{N-N}_2$) (Baggs, 2003; Bateman and
350 Baggs, 2005).

351

352 Soil cores were sampled from 0-10 cm for each habitat (n = 6 soil cores per habitat), with the
353 exception for upper montane forest, where two separate sets of cores were collected, one
354 from the organic layer (O horizon; n = 6) and the other from the mineral layer (A horizon; n =
355 6). Soil samples were then shipped to the University of Aberdeen and sampled within one
356 week of arrival. Transport times from Peru to the UK varied between one and two weeks.
357 Five of these soil cores, one for each replicate, were split into four equal parts (3 treatment
358 samples and one control sample) and distributed into 1 L screw top jars (Kilner, UK). A small
359 soil subsample from each core was used to determine WFPS, background NO_3^- content
360 (extracted in 100ml 1M KCl for a 10g soil sample prior to the start of the experiment), as well
361 as total C and N content. If necessary, the samples were gravimetrically amended with water
362 until the cores reached 80% WFPS. Soil cores were kept under constant conditions for 3 days
363 before the start of the experiment to minimize the effects of changing water content on soil
364 processes.

365

366 At the start of the experiment, dissolved ^{15}N -labelled KNO_3 (30 atom %) was added
367 according to the measured NO_3^- concentrations of each core to reach the required NO_3^-
368 concentration for each treatment (Table 2). Initial NO_3^- concentration (prior to ^{15}N addition)
369 averaged (\pm standard error) $157 \pm 12 \mu\text{g N g soil}^{-1}$ for pre-montane forest, $140 \pm 12 \mu\text{g N g}$
370 soil^{-1} for lower montane forest, $19 \pm 7 \mu\text{g N g soil}^{-1}$ for upper montane forest organic layer
371 soil, $18 \pm 5 \mu\text{g N g soil}^{-1}$ for upper montane forest mineral layer soil, and $6 \pm 2 \mu\text{g N g soil}^{-1}$ for
372 montane grassland soil (Table 2). The jars were then sealed with lids fitted with a two-way
373 stopcock to allow for gas sampling. Gas samples were taken with gas tight syringes, and
374 stored in pre-evacuated containers for determination of $^{15}\text{N-N}_2$, $^{15}\text{N-N}_2\text{O}$, N_2O , CO_2 and CH_4
375 content. Isotope samples (150 ml) were stored in 100 mL serum bottles and gas
376 concentration samples (20 ml) were stored in 12 ml Exetainers® (Labco Ltd., Lampeter, UK).
377 After gas sampling, the stopcock was opened to allow the sampled air from the jar to be
378 replaced by lab air, and lab air was sampled to allow for correction of the gas concentrations
379 in the jars due to dilution. Samples were taken at 0, 6, 12, 24, 36, and 48 hours, after which

380 the jars were opened and soil was sampled for determination of NO_3^- , NH_4^+ and total C and
381 N. Gas flux, isotopic and elemental concentrations were determined according to the
382 methods described previously.

383

384 **4.7 Statistics**

385 Statistical analyses were performed using JMP IN Version 8 (SAS Institute, Inc., Cary, North
386 Carolina, USA) or R (Team, 2012). Residuals were checked for heteroscedasticity and
387 homogeneity of variances. Where necessary, the data were transformed using a Box-Cox
388 procedure to meet the assumptions of analysis of variance. Analysis of variance (ANOVA) or
389 Generalized Linear Models were used to evaluate the effect of categorical variables (i.e. site,
390 season, topography) on trace gas flux and environmental variables. Analysis of covariance
391 (ANCOVA) was performed on Box-Cox transformed data to investigate the combined effects
392 of categorical variables and environmental factors (e.g. water-filled pore space, soil oxygen
393 content, air temperature, soil temperature, etc.) on trace gas flux. Non-parametric tests
394 were employed where Box-Cox transformation was unable to normalize the data,
395 homogenize the variances, or where the residuals still showed strong trends even after Box-
396 Cox transformation. Means comparisons were performed using Fisher's Least Significant
397 Difference test (Fisher's LSD). Statistical significance was determined at the $P < 0.05$ level,
398 unless otherwise noted. Values are reported as means and standard errors (± 1 SE).
399 Statistical analyses for the field data were conducted on plot-averaged data to avoid pseudo-
400 replication.

401

402

403 **5. Results**

404 **5.1 Variations in N_2O flux among habitats and between seasons**

405 The overall mean N_2O flux for the entire dataset was 0.27 ± 0.07 mg $\text{N-N}_2\text{O m}^{-2} \text{d}^{-1}$, with a
406 range from -8.40 to 75.0 mg $\text{N-N}_2\text{O m}^{-2} \text{d}^{-1}$. We investigated the effect of habitat, season,
407 topography, and the interaction of habitat by season on N_2O flux by using a three-way
408 ANOVA on plot-averaged data ($F_{10,307} = 3.28$, $P < 0.0005$; Supplementary Online Materials
409 Table S1A). We found that there was a significant effect of habitat ($P < 0.003$) and an effect
410 of season at the borderline of statistical significance ($P < 0.07$). However, we found no effect
411 of topography and no habitat by season interaction effect on N_2O flux. Habitat accounted for

412 the largest proportion of variance in the dataset (4.3 %), while season accounted for only 1.0
413 % of the variance (Supplementary Online Materials Table S1A).

414

415 Among habitats, the overall trend was towards the highest flux from premontane forest
416 ($0.75 \pm 0.18 \text{ mg N-N}_2\text{O m}^{-2} \text{ d}^{-1}$), followed by lower montane forest ($0.46 \pm 0.24 \text{ mg N-N}_2\text{O m}^{-2}$
417 d^{-1}), montane grasslands ($0.07 \pm 0.08 \text{ mg N-N}_2\text{O m}^{-2} \text{ d}^{-1}$), and upper montane forest ($0.04 \pm$
418 $0.07 \text{ mg N-N}_2\text{O m}^{-2} \text{ d}^{-1}$) (Figure 2a). Multiple comparisons tests indicated that only
419 premontane forests showed statistically higher flux than the others (Fisher's LSD, $P < 0.05$);
420 while there were numerical differences in mean flux among the other habitats, large
421 variances meant that they had overlapping ranges of flux (Figure 2a).

422

423 The borderline significant effect of season ($P < 0.07$) reflected an overall trend of higher dry
424 season ($0.51 \pm 0.18 \text{ mg N-N}_2\text{O m}^{-2} \text{ d}^{-1}$) compared to wet season flux ($0.15 \pm 0.07 \text{ mg N-N}_2\text{O}$
425 $\text{m}^{-2} \text{ d}^{-1}$) in the pooled dataset (Table 3). However, part of why the effect of season was weak
426 was because only lower montane forest showed significant variability between seasons
427 (Fisher's LSD, $P < 0.05$), while the other three habitats did not show significant seasonal
428 differences in flux (Fisher's LSD, $P < 0.05$).

429

430 Even though the effect of topography alone was not statistically significant, N_2O flux from
431 flat sites were significantly higher ($0.62 \pm 0.28 \text{ mg N-N}_2\text{O m}^{-2} \text{ d}^{-1}$) than from the basin site ($-$
432 $0.18 \pm 0.16 \text{ mg N-N}_2\text{O m}^{-2} \text{ d}^{-1}$) (Fisher's LSD, $P < 0.05$). However, there was no significant
433 difference between flat sites and either slope or ridge sites ($0.24 \pm 0.09 \text{ mg N-N}_2\text{O m}^{-2} \text{ d}^{-1}$ and
434 $0.20 \pm 0.08 \text{ mg N-N}_2\text{O m}^{-2} \text{ d}^{-1}$, respectively) (Fisher's LSD, $P > 0.05$).

435

436 For each habitat, we also compared individual wet and dry seasons against each other using
437 multiple comparisons tests (e.g. dry season 2012 vs wet season 2012; dry season 2012 vs dry
438 season 2013, etc.) to determine if there was significant inter-annual (i.e. year-on-year)
439 variation in N_2O flux among seasons. Consistent with our three-way ANOVA results, we
440 found that only lower montane forest showed significant variation among multiple dry and
441 wet seasons, whereas the other habitats showed no significant trends. For lower montane
442 forest, we observed significantly higher dry season flux in 2011 compared to wet and dry
443 seasons in all other years ($P < 0.05$; Figure 3b).

444

445 **5.2 Variations in environmental conditions among habitats and between seasons**

446 We investigated the effect of habitat, season, topography, and the interaction of habitat by
447 season on environmental variables using a three-way ANOVA on plot-averaged data. The
448 environmental variables examined here were: water-filled pore space (WFPS) in the 0-10 cm
449 depth, gas-phase soil oxygen content in the 0-10 cm depth, soil temperature, air
450 temperature, and resin-extractable inorganic N flux (NH_4^+ , NO_3^-).

451

452 Water-filled pore space varied significantly as a function of habitat, season, habitat by
453 season, and topography ($F_{10,304} = 637.96$, $P < 0.0001$; Table 3; Figure 2b; Figure 3;
454 Supplementary Online Materials Table S1B). Habitat accounted for the largest proportion of
455 variance in the model (78.1 %), followed by season (0.6 %), habitat by season interaction (0.6
456 %), and topography (0.4 %) (Supplementary Online Materials Table S1B). Each habitat
457 differed significantly from the others (Fisher's LSD, $P < 0.05$), with the highest WFPS observed
458 in montane grassland (88.4 ± 0.3 %), followed by premontane forest (51.6 ± 1.3 %), lower
459 montane forest (39.0 ± 0.9 %), and upper montane forest (35.0 ± 1.5 %) (Figure 2b). WFPS
460 varied significantly between seasons (t-Test, $P < 0.05$), with a mean dry season value of 52.1
461 ± 2.4 % compared to a mean wet season value of 59.5 ± 1.6 % (Table 3). The significant
462 habitat by season interaction is due to the fact that some habitats showed seasonal trends in
463 WFPS whereas others did not. Whereas lower montane and upper montane forests all
464 showed a significant reduction in WFPS during the dry season, premontane forest and
465 montane grasslands showed no seasonal differences in WFPS (Table 3, Figure 3). For
466 topography, the main effect was that the basin landform had significantly higher WFPS than
467 the other landforms. The basin landform showed a mean WFPS of 89.3 ± 0.1 % whereas
468 WFPS in other landforms ranged from 51.7 ± 2.2 to 57.7 ± 2.7 %.

469

470 Soil oxygen in the 0-10 cm depth varied significantly as a function of habitat, habitat by
471 season, and topography ($F_{10,242} = 27.70$, $P < 0.0001$; Table 3; Supplementary Online Materials
472 Table S1C). Habitat accounted for the largest proportion of variance in the model (66.9 % of
473 the total variance), followed by topography (8.4 %), habitat by season (3.5 %)
474 (Supplementary Online Materials Table S1C). For habitat, multiple comparisons tests
475 indicated that only montane grasslands showed significantly lower soil O_2 content than the

476 other habitats (13.5 ± 0.6 %), while the others showed statistically similar soil O₂ values to
477 each other (18.6 ± 0.2 to 19.5 ± 0.1 %; Fisher's LSD, $P < 0.05$). For topography, multiple
478 comparisons tests indicated that the basin landform showed statistically lower soil O₂
479 content than the other landforms (7.4 ± 2.3 %), whereas the other topographic features
480 showed statistically similar values, ranging from 16.9 ± 0.6 to 18.2 ± 0.2 % (Fisher's LSD, $P <$
481 0.05). The significant habitat by season interaction was due to the fact that only montane
482 grassland showed a significant difference in O₂ content between wet and dry season,
483 whereas other habitats showed similar soil O₂ values (Table 3).

484

485 For soil temperature, the effects of habitat, season, habitat by season, and topography were
486 all significant ($F_{10,292} = 790.7$, $P < 0.0001$; Supplementary Online Materials Table S1D).
487 Habitat accounted for the largest proportion of variance in the model (85.5 % of the total
488 variance), followed by season (1.4%), habitat by season interaction (0.5 %), and topography
489 (0.3 %) (Supplementary Online Materials Table S1D). Each habitat differed significantly from
490 the others (Fisher's LSD, $P < 0.05$), with the highest soil temperature observed for
491 premontane forest (20.5 ± 0.1 °C), followed by lower montane forest (17.8 ± 0.1 °C), upper
492 montane forest (11.5 ± 0.1 °C), and montane grasslands (10.6 ± 0.2 °C). Soil temperature
493 varied significantly between season (t-Test, $P < 0.05$), with a mean dry season value of $13.9 \pm$
494 0.4 °C compared to a mean wet season value of 15.1 ± 0.3 °C. The significant habitat by
495 season interaction is due to the fact that some habitats showed more pronounced seasonal
496 trends in soil temperature than others, although the overall pattern of cooler dry season
497 compared to wet season soil temperatures holds across all habitats (Table 3). For
498 topography, the flat landforms showed significantly higher soil temperatures than the others
499 (16.0 ± 0.5 °C), the basin landform showed significantly lower values (10.8 ± 0.4 °C), whereas
500 ridge and slope landforms showed similar values to each other (14.3 ± 0.4 °C and 14.7 ± 0.4
501 °C, respectively) (Fisher's LSD, $P < 0.05$).

502

503 For air temperature, only the effect of habitat was significant ($F_{10,292} = 103.2$, $P < 0.0001$;
504 Table 3; Supplementary Online Materials Table S1E). A multiple comparisons test indicated
505 that each habitat showed significantly different temperatures compared to the others
506 (Fisher's LSD, $P < 0.05$). Premontane forest showed the highest air temperatures (21.0 ± 0.3
507 °C), followed by lower montane forest (18.7 ± 0.2 °C), upper montane forest (12.7 ± 0.2 °C),

508 and montane grassland (11.7 ± 0.3 °C). Other variables did not significantly affect air
509 temperature.

510

511 For resin-extractable NH_4^+ flux, even though the three-way ANOVA model was not
512 statistically significant, the overall trend was towards significantly lower NH_4^+ flux in the dry
513 season (9.6 ± 0.7 $\mu\text{g N-NH}_4$ $\text{g resin}^{-1} \text{d}^{-1}$) compared to the wet season (22.3 ± 3.6 $\mu\text{g N-NH}_4$
514 $\text{g resin}^{-1} \text{d}^{-1}$) ($F_{10,164} = 1.3$, $P > 0.2$; Table 3; Supplementary Online Materials Table S1F).

515

516 Resin-extractable NO_3^- flux showed different patterns from NH_4^+ flux, with significant effects
517 of habitat, topography, and habitat by season but not of season alone ($F_{10,164} = 39.0$, $P <$
518 0.0001 ; Figure 2c; Table 3; Supplementary Online Materials Table S1G). Habitat accounted
519 for the largest proportion of the variance (61.5 %), followed by topography (4.7 %), and
520 habitat by season (1.9 %). Premontane forest showed the highest NO_3^- flux (22.6 ± 2.0 $\mu\text{g N-NO}_3$
521 $\text{g resin}^{-1} \text{d}^{-1}$), followed by lower montane forest (10.0 ± 1.2 $\mu\text{g N-NO}_3$ $\text{g resin}^{-1} \text{d}^{-1}$)
522 (Fisher's LSD, $P < 0.05$; Figure 2c). Upper montane forest (1.1 ± 0.2 $\mu\text{g N-NO}_3$ $\text{g resin}^{-1} \text{d}^{-1}$) and
523 montane grassland (1.7 ± 0.3 $\mu\text{g N-NO}_3$ $\text{g resin}^{-1} \text{d}^{-1}$) showed significantly lower NO_3^- flux than
524 the other two habitats (Fisher's LSD, $P < 0.05$; Figure 2c), with values that were not
525 significantly different from each other (Fisher's LSD, $P > 0.05$; Figure 2c). For the effect of
526 topography, multiple comparisons tests indicated that flat landforms (12.1 ± 1.8 $\mu\text{g N-NO}_3$ g
527 $\text{resin}^{-1} \text{d}^{-1}$) and slope landforms (10.2 ± 1.6 $\mu\text{g N-NO}_3$ $\text{g resin}^{-1} \text{d}^{-1}$) differed significantly from
528 ridge landforms (6.6 ± 1.4 $\mu\text{g N-NO}_3$ $\text{g resin}^{-1} \text{d}^{-1}$) (Fisher's LSD, $P < 0.05$). The basin landform
529 (3.8 ± 1.3 $\mu\text{g N-NO}_3$ $\text{g resin}^{-1} \text{d}^{-1}$), despite the lower mean values, showed an overlapping
530 range with the other landforms (Fisher's LSD, $P > 0.05$). The habitat by season interaction
531 was due to the fact that upper montane forest shows a significant seasonal fluctuation in
532 resin-extractable NO_3^- (Fisher's LSD, $P < 0.05$), whereas the other habitats show no significant
533 seasonal trend (Fisher's LSD, $P > 0.05$; Table 3).

534

535 **5.3 Effects of environmental variables on N_2O flux**

536 For the whole dataset, the relationship between N_2O flux and environmental variables was
537 examined using an ANCOVA on Box-Cox transformed data with habitat, season, topography,
538 and environmental variables as covariates. Environmental variables included WFPS, oxygen,
539 air temperature, soil temperature, and resin-extractable inorganic N flux (NH_4^+ and NO_3^-).

540 The ANCOVA model as a whole was not statistically significant ($P > 0.4$). However, we found
541 that individual factors were weakly but significantly correlated with N_2O flux for the pooled
542 dataset. These included soil temperature ($r^2 = 0.04$, $P < 0.0004$), air temperature ($r^2 = 0.04$, P
543 < 0.0008), and resin-extractable NO_3^- flux ($r^2 = 0.03$, $P < 0.03$). Water-filled pore space also
544 showed a very weak negative correlation with N_2O flux at the borderline of statistical
545 significance ($r^2 = 0.01$, $P < 0.06$).

546
547 For individual habitats, we explored how variations in environmental conditions influenced
548 N_2O flux using multiple regression, with WFPS, oxygen, soil temperature, air temperature,
549 resin-extractable NH_4^+ flux, and resin-extractable NO_3^- flux as explanatory variables. Only the
550 multiple regression analysis for lower montane forest showed a borderline significant result,
551 though only at the $P < 0.07$ level ($r^2 = 0.36$). The multiple regression models for all the other
552 habitats were not statistically significant ($P > 0.4$). Lower montane forest was the only
553 habitat that showed a significant effect of season on N_2O flux (section 5.1), and our multiple
554 regression model corroborated this result by showing that seasonal fluctuations in air
555 temperature, soil temperature, WFPS (Figure 3b), and NH_4^+ all correlated with N_2O flux ($P <$
556 0.05). Air temperature explained the largest proportion of variance in the data (26.2 %;
557 negative trend), followed by soil temperature (15.5 %; positive trend), WFPS (13.7 %;
558 negative trend), and resin-extractable NH_4^+ flux (11.6 %; negative trend).

559

560 **5.4 Water-filled pore space manipulation**

561 ^{15}N - N_2O and ^{15}N - N_2 fluxes showed a biphasic response (Limmer and Steele, 1982), with
562 significantly different flux rates in the first 24 hours of incubation compared to the later
563 period of incubation (i.e. 24-48 hours). Flux of ^{15}N - N_2O , and ^{15}N - N_2 were therefore divided
564 into early (0-24 hours) and late (24-48 hours) phase flux.

565

566 **5.4.1 Role of nitrification and nitrate reduction in N_2O production**

567 The ^{15}N flux data indicates that nitrate reduction (i.e. denitrification) was the dominant
568 source of N_2O from these soils, while nitrification was only a minor contributor to ^{15}N - N_2O
569 production (Supplementary Online Materials Figure S1). The ^{15}N - N_2O and ^{15}N - N_2 fluxes were
570 analyzed using a full factorial ANOVA on Box-Cox transformed data with habitat, moisture
571 level, form of ^{15}N -label added (i.e. $^{15}\text{NH}_4^{15}\text{NO}_3$ or $^{14}\text{NH}_4^{15}\text{NO}_3$), incubation phase, and all their

572 interaction terms as independent variables. Notably, this analysis revealed that the form of
573 ^{15}N -label added (i.e. $^{15}\text{N-NH}_4^{15}\text{N-NO}_3$ or $^{14}\text{N-NH}_4^{15}\text{N-NO}_3$) did not significantly alter $^{15}\text{N-N}_2\text{O}$
574 flux, indicating that production of $^{15}\text{N-N}_2\text{O}$ from nitrification was weak to negligible
575 (Supplementary Online Materials Figure S1). In order to simplify our statistical analyses, all
576 subsequent analyses were performed using only habitat, moisture level, incubation phase,
577 and their interaction terms as independent variables. For these tests, which are described
578 below, the “total” flux of $^{15}\text{N-N}_2\text{O}$ or $^{15}\text{N-N}_2$ represents gas produced by both nitrification
579 and nitrate reduction.

580

581 **5.4.2 $^{15}\text{N-N}_2\text{O}$ flux**

582 For the total $^{15}\text{N-N}_2\text{O}$ flux data, we used a full factorial ANOVA on Box-Cox transformed data
583 with habitat, moisture level, incubation phase, and all their interactions as independent
584 variables. We found that moisture level, habitat by incubation phase, and habitat by
585 moisture by incubation phase were significantly related to $^{15}\text{N-N}_2\text{O}$ flux (ANOVA, $F_{31, 321} =$
586 3.06 , $P < 0.0001$; Figure 4; Supplementary Online Materials Table S2A). Of the three main
587 factors (i.e. habitat, moisture level, incubation phase), moisture level was the dominant
588 control on $^{15}\text{N-N}_2\text{O}$ flux (Supplementary Online Materials Table S2A). The highest $^{15}\text{N-N}_2\text{O}$
589 flux was observed in the 90 % WFPS ($42 \pm 9 \text{ ng N}_2\text{O-}^{15}\text{N g}^{-1} \text{ d}^{-1}$) and 50 % WFPS ($29 \pm 10 \text{ ng}$
590 $\text{N}_2\text{O-}^{15}\text{N g}^{-1} \text{ d}^{-1}$) treatments, and the lowest flux in the 30 % ($3 \pm 1 \text{ ng N}_2\text{O-}^{15}\text{N g}^{-1} \text{ d}^{-1}$) and 70
591 % ($7 \pm 2 \text{ ng N}_2\text{O-}^{15}\text{N g}^{-1} \text{ d}^{-1}$) treatments (Fisher’s LSD, $P < 0.05$; Figure 4). The habitat by
592 incubation phase interaction indicated that some habitats showed different flux rates during
593 early and late phases of the incubation (Figure 4). Premontane and lower montane forest
594 showed statistically similar $^{15}\text{N-N}_2\text{O}$ flux during early and late incubation phases. Upper
595 montane forest mineral layer soils showed a significant increase in $^{15}\text{N-N}_2\text{O}$ flux from early to
596 late incubation phases ($5 \pm 2 \text{ ng N}_2\text{O-}^{15}\text{N g}^{-1} \text{ d}^{-1}$ versus $42 \pm 13 \text{ ng N}_2\text{O-}^{15}\text{N g}^{-1} \text{ d}^{-1}$; t-Test, $P <$
597 0.003), while montane grasslands showed a significant decrease in $^{15}\text{N-N}_2\text{O}$ flux from early to
598 late incubation phases ($60 \pm 23 \text{ ng N}_2\text{O-}^{15}\text{N g}^{-1} \text{ d}^{-1}$ versus $6 \pm 9 \text{ ng N}_2\text{O-}^{15}\text{N g}^{-1} \text{ d}^{-1}$, respectively;
599 t-Test, $P < 0.02$). The habitat by moisture by incubation phase effect stems from complex
600 and varying responses of soils from different habitats to differences in moisture level and
601 incubation phase (Figure 4).

602

603 **5.4.3 $^{15}\text{N-N}_2$ flux**

604 For the total $^{15}\text{N-N}_2$ flux data, we used a full factorial ANOVA on Box-Cox transformed data
605 with habitat, moisture level, incubation phase, and all their interactions as independent
606 variables. We found that all of the main factors and their interaction terms were statistically
607 significant (ANOVA, $F_{31, 317} = 14.20$, $P < 0.0001$; Supplementary Online Materials Table S2B).
608 Of the three main factors, habitat was the dominant control on $^{15}\text{N-N}_2$ flux (Supplementary
609 Online Materials Table S2B). Lower montane forest showed the highest $^{15}\text{N-N}_2$ flux (694 ± 83
610 $\text{ng N}_2\text{-}^{15}\text{N g}^{-1} \text{d}^{-1}$); premontane forest and upper montane forest mineral layer soil showed
611 intermediate levels of flux (326 ± 53 and $171 \pm 20 \text{ ng N}_2\text{-}^{15}\text{N g}^{-1} \text{d}^{-1}$, respectively); and
612 montane grassland soil showed the lowest flux ($123 \pm 23 \text{ ng N}_2\text{-}^{15}\text{N g}^{-1} \text{d}^{-1}$) (Fisher's LSD, $P <$
613 0.05 ; Figure 4). Moisture played a secondary role in regulating $^{15}\text{N-N}_2$ flux (Supplementary
614 Online Materials Table S2B), with only the 90 % treatment had significantly higher flux than
615 the other treatments (90 % WFPS treatment: $437 \pm 77 \text{ ng N}_2\text{-}^{15}\text{N g}^{-1} \text{d}^{-1}$; pooled average for
616 all other treatments: $294 \pm 28 \text{ ng N}_2\text{-}^{15}\text{N g}^{-1} \text{d}^{-1}$) (Fisher's LSD, $P < 0.05$). Incubation phase was
617 the least important control on $^{15}\text{N-N}_2$ flux, with slightly greater flux of $^{15}\text{N-N}_2$ during the late
618 compared to the early phase of the incubations ($373 \pm 44 \text{ ng N}_2\text{-}^{15}\text{N g}^{-1} \text{d}^{-1}$ versus $288 \pm 37 \text{ ng}$
619 $\text{N}_2\text{-}^{15}\text{N g}^{-1} \text{d}^{-1}$) (t-Test, $P < 0.07$). The habitat by moisture level interaction indicates that flux
620 from different habitats showed varying moisture responses (Figure 4). For example, $^{15}\text{N-N}_2$
621 flux from premontane forest and upper montane forest mineral layer soil showed no
622 responses to moisture. In contrast, for lower montane forest, flux was greatest for the 90 %
623 WFPS treatment ($1,365 \pm 201 \text{ ng N}_2\text{-}^{15}\text{N g}^{-1} \text{d}^{-1}$), lowest for the 70 % WFPS treatment ($257 \pm$
624 $128 \text{ ng N}_2\text{-}^{15}\text{N g}^{-1} \text{d}^{-1}$), and at intermediate levels for the 30 and 50 % WFPS treatments ($664 \pm$
625 131 and $492 \pm 79 \text{ ng N}_2\text{-}^{15}\text{N g}^{-1} \text{d}^{-1}$, respectively) (Fisher's LSD, $P < 0.05$). The pattern for
626 montane grassland was different again; here, only the 90 % WFPS treatment showed
627 significantly greater flux ($171 \pm 32 \text{ ng N}_2\text{-}^{15}\text{N g}^{-1} \text{d}^{-1}$) compared to the other treatments
628 (pooled average: $105 \pm 29 \text{ ng N}_2\text{-}^{15}\text{N g}^{-1} \text{d}^{-1}$) (Fisher's LSD, $P < 0.05$).

629

630 5.4.4 N_2O Yield

631 For the N_2O yield, we used a full factorial ANOVA on Box-Cox transformed data with habitat,
632 moisture level, incubation phase, and all their interactions as independent variables. We
633 found that habitat, moisture level, habitat by moisture level, habitat by phase, and habitat
634 by moisture level by phase significantly influenced N_2O yield (ANOVA, $F_{31, 313} = 9.85$, $P <$
635 0.0001 ; Supplementary Online Materials Table S2C). Of the three main factors, habitat was

636 the best predictor of N₂O yield (Supplementary Online Materials Table S2C). N₂O yield was
637 highest for the montane grassland (0.61 ± 0.06), lowest for lower montane forest (0.19 ±
638 0.04), while premontane forest and upper montane forest mineral layer soil showed similar
639 intermediate values (0.40 ± 0.05 and 0.42 ± 0.05, respectively) (Fisher's LSD, *P* < 0.05).
640 Moisture level explained much less of the variance in the dataset (Supplementary Online
641 Materials Table S2C); N₂O yield was highest for the 70 % WFPS treatment (0.51 ± 0.06), while
642 the 30, 50 and 90 % WFPS treatments showed statistically similar values (0.35 ± 0.05, 0.39 ±
643 0.05, and 0.36 ± 0.05, respectively) (Fisher's LSD, *P* < 0.05). For the habitat by moisture level
644 interaction, this reflects the fact that only lower montane forest and upper montane forest
645 showed differences in N₂O yield with changes in moisture level. For the lower montane
646 forest, N₂O yield was greatest in the 70 % WFPS treatment (0.51 ± 0.11), whereas the other
647 treatments were not statistically different from each other (pooled average: 0.09 ± 0.03)
648 (Fisher's LSD, *P* < 0.05). Upper montane forest mineral layer soil showed the highest N₂O
649 yield for the 90 % treatment (0.72 ± 0.08), lowest yield for the 30 % WFPS treatment (0.20 ±
650 0.09), and intermediate N₂O yields for the 50 and 70 % WFPS treatments (0.29 ± 0.09 and
651 0.50 ± 0.11, respectively) (Fisher's LSD, *P* < 0.05). For the habitat by incubation phase
652 interaction, this reflects the fact that upper montane forest mineral layer soil showed an
653 increase in N₂O yield from early to late phase, while montane grassland showed a decrease
654 in N₂O yield from early to late phase. The habitat by moisture level by incubation phase
655 interaction reflects the complex and varied responses of soils from different habitats to
656 changes in moisture level and incubation phase (Figure 4).

657

658 **5.5 Litter manipulation experiment**

659 In order to investigate the relationship between leaf litter input rates and N₂O flux, we used
660 a Generalized Linear Model (GLM) and an ANCOVA that included habitat, litter treatment,
661 season, WFPS, litter input rate, litter C input rate, litter N input rate, soil temperature and air
662 temperature as independent variables. The analysis was also repeated using ANCOVA on
663 Box-Cox transformed data. Both analyses revealed no significant statistical relationship
664 between N₂O flux and any of these environmental variables, with the exception of soil
665 temperature, which showed only a weak positive relationship to N₂O flux when the data was
666 analysed using the GLM (*P* < 0.05). This relationship was not detected using ANCOVA.

667 Bivariate regression of soil temperature against N₂O flux indicated that the relationship was
668 relatively weak, with $r^2 = 0.01$ ($P < 0.05$).

669

670 **5.6 Nitrate addition experiment**

671 ¹⁵N-N₂O and ¹⁵N-N₂ fluxes showed a biphasic response (Limmer and Steele, 1982), with
672 significantly different flux rates in the first 24 hours of incubation compared to the later
673 period of incubation (i.e. 24-48 hours). Flux of ¹⁵N-N₂O, and ¹⁵N-N₂ were therefore divided
674 into early (0-24 hours) and late (24-48 hours) phase flux.

675

676 **5.6.1 ¹⁵N-N₂O flux**

677 For the ¹⁵N-N₂O flux data, we used a full factorial ANOVA on Box-Cox transformed data with
678 habitat, N addition level, incubation phase, and all their interaction terms as independent
679 variables. Habitat, incubation phase, and the habitat by incubation phase interaction all
680 significantly influenced ¹⁵N-N₂O flux (ANOVA, $F_{29, 149} = 5.67$, $P < 0.0001$; Figure 5;
681 Supplementary Online Materials Table S3A). Notably, N addition level did not significantly
682 influence ¹⁵N-N₂O flux. Of the three main factors (i.e. habitat, N addition level, incubation
683 phase), habitat was the best predictor of ¹⁵N-N₂O flux, explaining a largest proportion of the
684 variance (Supplementary Online Materials Table S3A). Upper montane forest organic layer
685 soils showed the highest flux (238 ± 160 ng N₂O-¹⁵N g⁻¹ d⁻¹), lower montane (179 ± 48 ng
686 N₂O-¹⁵N g⁻¹ d⁻¹) and premontane (86 ± 16 ng N₂O-¹⁵N g⁻¹ d⁻¹) forest showed intermediate flux,
687 while montane grasslands (11 ± 4 ng N₂O-¹⁵N g⁻¹ d⁻¹) and upper montane forest mineral layer
688 soils (0.06 ± 0.01 ng N₂O-¹⁵N g⁻¹ d⁻¹) showed the lowest flux (Fisher's LSD, $P < 0.05$). The
689 effect of incubation phase was attributable to significantly greater ¹⁵N-N₂O flux during the
690 late compared to early incubation phases (164 ± 66 ng N₂O-¹⁵N g⁻¹ d⁻¹ versus 42 ± 11 ng N₂O-
691 ¹⁵N g⁻¹ d⁻¹; t-Test, $P < 0.05$; Figure 5). The habitat by incubation phase interaction was caused
692 by some habitats showing higher flux in certain incubation phases than others (Figure 5).
693 During the early phase, lower montane and premontane forests collectively showed the
694 highest flux (Figure 5; Fisher's LSD, $P < 0.05$). In contrast, during the late incubation phase,
695 upper montane forest organic layer soils, lower montane forest, and premontane forest now
696 showed the highest flux (Figure 5; Fisher's LSD, $P < 0.05$).

697

698 **5.6.2 ¹⁵N-N₂ flux**

699 For the ^{15}N - N_2 flux data, we used a full factorial ANOVA on Box-Cox transformed data with
700 habitat, N addition level, incubation phase, and all their interaction terms as independent
701 variables. Only habitat significantly influenced flux, while other terms were not significant
702 (ANOVA, $F_{29, 149} = 1.66$, $P < 0.05$; Figure 5; Supplementary Online Materials Table S3B). Lower
703 montane and upper montane forest organic layer soils showed the highest flux (472 ± 139
704 and $576 \pm 117 \text{ ng N}_2\text{-}^{15}\text{N g}^{-1} \text{ d}^{-1}$, respectively), while all other habitats showed similar flux
705 rates ($105 \pm 19 \text{ ng N}_2\text{-}^{15}\text{N g}^{-1} \text{ d}^{-1}$) (Fisher's LSD, $P < 0.05$; Figure 5).

706

707 **5.6.3 N_2O Yield**

708 For the N_2O yield, we used a full factorial ANOVA on Box-Cox transformed data with habitat,
709 N addition level, incubation phase (i.e. early versus late), and all their interaction terms as
710 independent variables. We found that none of these factors predicted N_2O yield (ANOVA,
711 $F_{29, 149} = 0.75$, $P > 0.82$; Supplementary Online Materials Table S3C). The overall mean N_2O
712 yield for the pooled dataset was 0.53 ± 0.04 .

713

714

715 **6. Discussion**

716 **6.1 Effects of seasonality and soil moisture on N_2O flux**

717 Nitrous oxide flux in the Kosñipata Valley showed weak seasonality, with greater N_2O flux
718 during the dry season compared to the wet season. This regional trend was consistent with
719 results from our prior study, and was principally driven by strong seasonality in N_2O flux
720 from lower montane forest (Teh et al., 2014). In contrast, other habitats showed little or no
721 seasonal variation in N_2O flux. This weak seasonality in N_2O flux across the Kosñipata Valley
722 probably stems from relatively modest variation in environmental variables among seasons
723 (Table 3), in accordance with observations from elsewhere in the Andes (Baldos et al.,
724 2015; Müller et al., 2015; Wolf et al., 2011). For example, while soil moisture (i.e. WFPS)
725 varied significantly between seasons in the dataset as a whole, the absolute difference in
726 WFPS between dry season and wet season were relatively small (i.e. 7.4 %). Indeed, some
727 habitats showed much smaller variations in soil moisture, such as premontane forest and
728 montane grassland that showed no significant seasonal variation in WFPS whatsoever (Table
729 3).

730

731 One critical factor contributing to these weak seasonal trends in N₂O flux is the atypical
732 response of N₂O flux to changes in soil moisture. Nitrous oxide flux showed a weak but
733 negative correlation with WFPS in the field dataset ($r^2= 0.01$, $P < 0.06$ for the pooled dataset),
734 rather than following a curvilinear pattern predicted by denitrification theory (Firestone and
735 Davidson, 1989; Firestone et al., 1980; Weier et al., 1993; Davidson, 1991). Likewise, in our soil
736 moisture manipulation experiments, nitrification made a minor contribution to N₂O
737 production, irrespective of soil moisture content (Supplementary Online Materials Figure
738 S1). This finding is contrary to theoretical predictions of N₂O production by ammonia-
739 oxidizing bacteria (AOB), where N₂O production from ammonia-oxidation is thought to make
740 an important contribution to N₂O flux at lower soil moisture contents (i.e. 30-60 % WFPS)
741 (Firestone and Davidson, 1989; Firestone et al., 1980; Weier et al., 1993; Davidson, 1991). At
742 higher soil moisture contents (i.e. >60 % WFPS), N₂O flux showed a non-linear response to
743 increasing WFPS, with two distinct peaks in N₂O flux at 90 and 50 % WFPS (Figure 4).
744 Collectively, these findings suggest that the role of soil moisture in regulating N₂O flux is
745 more complex than predicted by existing theory, falsifying our first two hypotheses.

746

747 What could explain these unexpected trends? We believe that these patterns occurred due
748 to the complex interplay between environmental conditions and the microbial processes
749 that produce N₂O in soil (i.e. ammonia oxidation by archaea, ammonia oxidation by bacteria,
750 denitrification, dissimilatory nitrate reduction to ammonium). We suspect that the action of
751 lesser-known microbial processes, such as oxidation of ammonia by archaea and
752 dissimilatory nitrate reduction to ammonium (DNRA), may explain the divergence from
753 theoretical norms. Our expectations of how N₂O production should respond to variations in
754 soil moisture are predicated on the assumption that N₂O is produced almost exclusively by
755 AOB and denitrifying bacteria, with the former operating at lower soil moisture content (i.e.
756 30-60 % WFPS) and the latter at higher soil moisture content (i.e. >60 % WFPS) (Firestone
757 and Davidson, 1989; Firestone et al., 1980; Weier et al., 1993; Davidson, 1991). More recent
758 advances in soil N research, however, have highlighted the importance of other microbial
759 taxa or processes, not previously considered in conceptual or process-based models. For
760 example, recent work in acidic soils have demonstrated that ammonia oxidizing archaea
761 (AOA) play a more important role than AOB in ammonia oxidation, but produce significantly
762 less N₂O due to differences in metabolism (Hink et al., 2016; Prosser and Nicol, 2008).

763 Likewise, under higher soil moisture conditions (>60 % WFPS), DNRA – a process that
764 produces substantially less N₂O than denitrification and which also competes for NO₃⁻ with
765 denitrification – can dominate nitrate reduction, depending on redox conditions and the
766 relative availability of labile C and N (Morley and Baggs, 2010;Pett-Ridge and Firestone,
767 2005;Silver et al., 2001;Baldos et al., 2015;Müller et al., 2015). Thus, given the low pH of the
768 soils in Kosñipata Valley (Table 1), it is likely that AOA dominate ammonia oxidation at lower
769 levels of soil moisture, explaining the negligible amounts of N₂O produced from nitrification
770 in the 30 and 50 % WFPS treatments. As soils become wetter, the non-linear response of
771 N₂O flux to increasing soil moisture may reflect competition for substrates (e.g. NO₃⁻,
772 reducing equivalents) between DNRA and denitrification (Morley and Baggs, 2010;Silver et
773 al., 2001), or may indicate that DNRA is making a larger contribution to N₂O flux than
774 denitrification (Streminska et al., 2012).

775

776 These findings are important and noteworthy, given that climatically-driven variations in soil
777 moisture content are thought to be one of the dominant drivers for N₂O flux in the
778 seasonally dry tropics (Davidson, 1991;Firestone and Davidson, 1989;Groffman et al.,
779 2009;Davidson and Verchot, 2000;Teh et al., 2014;van Lent et al., 2015;Werner et al., 2007).
780 Moreover, similar results from comparable research sites in the Ecuadorian Andes lend
781 credence to our claims (Baldos et al., 2015;Müller et al., 2015). For example, Müller et al.
782 (2015) found that nitrification produced little or no N₂O in acidic Ecuadorian soils, in
783 agreement with findings from in this study. Likewise, ¹⁵N isotope pool dilution experiments,
784 in comparable habitats and elevations to our own, revealed that DNRA played a significant
785 role in nitrate reduction, supporting the notion that DNRA may represent a substantial sink
786 for NO₃⁻ in Peruvian soils (Baldos et al., 2015;Müller et al., 2015). Existing process-based
787 models, which are used to construct bottom-up emissions inventories for the tropics
788 (Werner et al., 2007), often assume that N₂O is derived primarily from AOB and
789 denitrification, with moisture response curves based on existing theoretical relationships (Li
790 et al., 2000;Werner et al., 2007;Smith et al., 2007). However, if these more “normative” soil
791 moisture response curves are inapplicable to montane tropical ecosystems, due to the
792 activity of AOA and DNRA, then a re-conceptualisation of the soil moisture-N₂O flux
793 relationship may be required. Moreover, if weak seasonality or aseasonality in N₂O flux is
794 the norm in Andean ecosystems (Müller et al., 2015;Wolf et al., 2011), then this finding may

795 have wider implications for understanding spatial or temporal trends in regional
796 atmospheric budgets (Kort et al., 2011; Nevison et al., 2004; Nevison et al., 2007; Saikawa et
797 al., 2014).

798

799 **6.2 Role of substrate limitation in regulating N₂O flux**

800 In accordance with our earlier work (Teh et al., 2014) and research conducted in analogous
801 ecosystems in Ecuador (Baldos et al., 2015; Müller et al., 2015; Wolf et al., 2011), we found
802 strong evidence that N₂O flux was constrained by the availability of NO₃⁻, partially supporting
803 our third hypothesis. In contrast, N₂O flux was unresponsive to short-term changes in labile
804 organic matter (i.e. leaf litter-fall) inputs, indicating that N₂O flux and nitrate reduction were
805 not C limited. This latter result is significant for modelling and extrapolating N₂O flux from
806 these habitats, because many process-based models assume that N cycling and turnover of
807 labile organic matter are intimately linked through processes such as litter production and
808 decomposition (Li et al., 2000; Werner et al., 2007; Smith et al., 2007).

809

810 Evidence for NO₃⁻ limitation of N₂O flux comes from both our field and laboratory data, and
811 suggests that “habitat” may be a good proxy for NO₃⁻ availability and N₂O flux because these
812 two variables co-vary with habitat. For example, we observed an inverse trend in field N₂O
813 flux, with premontane forest showing significantly greater flux than the other habitats
814 elevation (Table 3, Figure 2a). This inverse trend was also reflected in the resin-extractable
815 NO₃⁻ flux measured in the field and the ¹⁵N-N₂O flux measured in the NO₃⁻ addition
816 experiment in the laboratory (Figure 2c, 5a). Furthermore, the behaviour of the ¹⁵N-NO₃⁻
817 amended soils during the early (≤24 hours) and late (>24 hours) phases of the incubation
818 experiment suggest that soils from more N-poor habitats (i.e. those with lower rates of
819 resin-extractable NO₃⁻ flux; Table 3, Figure 2c) showed a greater proportional increase in ¹⁵N-
820 N₂O flux following NO₃⁻ addition than N-rich habitats (i.e. those with higher rates of resin-
821 extractable NO₃⁻ flux; Table 3, Figure 2c), suggesting that ¹⁵N-N₂O flux was more NO₃⁻ limited
822 in N-poor soils (Figure 5). Soils from the upper montane forest organic layer, montane
823 grasslands, and upper montane forest mineral layer showed the lowest ¹⁵N-N₂O flux during
824 the early phase of soil incubation, but the greatest proportional increase in flux during the
825 late phase of soil incubation, rising by a factor of 59, five, and two, respectively. In contrast,
826 lower montane and premontane forest soils showed the smallest proportional increase in

827 the late phase of soil incubation (i.e. 1.7 times increase). Last, the relatively low N₂O yield
828 observed in our soil moisture manipulations is thought to be broadly indicative of low NO₃⁻
829 conditions (i.e. <0.42 for forested habitats; Table 4), further supporting the notion that N₂O
830 flux in this region is generally NO₃⁻ limited (Schlesinger, 2009; Fang et al., 2015; Weier et al.,
831 1993).

832

833 Interestingly, ~~increasing NO₃⁻ availability per se did not stimulate ¹⁵N-N₂O flux, ¹⁵N-N₂ flux, or~~
834 ~~alter N₂O yield during the early phase (<24 hours) of the NO₃⁻ addition experiment, even~~
835 ~~though we did observe that ¹⁵N-N₂O flux did increase during the late phase (>24 hours) of~~
836 ~~the experiments (please see Figure 5 and discussion in the preceding paragraph).~~ Rather,
837 ANCOVA suggests that ¹⁵N-N₂O and ¹⁵N-N₂ fluxes ~~in the early phase of the NO₃⁻ addition~~
838 ~~experiment~~ were better-predicted by habitat; ~~i.e. that soil provenance was a better~~
839 ~~predictor of ¹⁵N-N₂O flux than N treatment~~. N₂O yield, normally a sensitive indicator of NO₃⁻
840 availability (Blackmer and Bremner, 1978; Weier et al., 1993; Parton et al., 1996), ~~also~~ showed
841 no immediate response to the amount of ¹⁵N-NO₃⁻ added, nor any of the other explanatory
842 variables. One explanation for this, consistent with the notion that N₂O flux is NO₃⁻ limited, is
843 that nitrate-reducing microbes in these soils may have a relatively low half-saturation
844 constant (*K_m*) for NO₃⁻, and effectively utilize NO₃⁻ whenever concentrations increase above
845 baseline (i.e. non-limiting) levels (Holtan-Hartwig et al., 2000). As a consequence, we may be
846 unable to differentiate among NO₃⁻ treatments ~~in the early phase of the experiment,~~
847 because the ~~amount of NO₃⁻ added~~ exceeded the *K_m* for these soils. This finding is also in
848 agreement with results from long-term N fertilization studies, which suggest that
849 substantive shifts in N₂O flux are only likely to occur after prolonged exposure to high levels
850 of N (i.e. >1 year), rather than due to transient fluctuations in N availability (Baldos et al.,
851 2015; Corre et al., 2010; Müller et al., 2015; Hall and Matson, 1999; Koehler et al., 2012).

852

853 6.3 Implications for annual atmospheric budgets and gaseous N loss

854 Montane ecosystems in the Kosñipata Valley were net sources of atmospheric N₂O, affirming
855 our prior results (Teh et al., 2014). The flux for this multi-annual dataset was comparable to
856 the preliminary values reported in our earlier publication, with an unweighted mean flux of
857 0.27 ± 0.07 mg N-N₂O m⁻² d⁻¹ observed over a 30 month period compared to 0.22 ± 0.12 mg
858 N-N₂O m⁻² d⁻¹ recorded over a 13 month period (Teh et al., 2014). These values correspond

Deleted:

Deleted: we found no evidence that these soils responded to short-term increases in NO₃⁻ availability, at least within the concentration range used for the experiments described here.

Deleted: and

Deleted: were not directly influenced by the amount of ¹⁵N-NO₃⁻ added

Deleted: .

Deleted: addition levels that we used all

869 to unweighted mean annual fluxes of $0.99 \pm 0.26 \text{ kg N}_2\text{O-N ha}^{-1} \text{ year}^{-1}$ and $0.80 \pm 0.44 \text{ kg}$
870 $\text{N}_2\text{O-N ha}^{-1} \text{ year}^{-1}$, respectively. However, in order to derive more accurate estimates of the
871 annual contribution of the Kosñipata Valley to the regional atmospheric budget of N_2O , it is
872 necessary to account for differences in land area for different habitats and variation in the
873 magnitude of N_2O flux between seasons. Thus, we conducted a simple weighted upscaling
874 exercise to more fully account for these two sources of variation (Table 4). Using the N_2O
875 yield data from the laboratory tracer experiments, we also estimated the annual N_2 flux and
876 total gaseous N flux, in order compare rates of gaseous N export from this region with other
877 forested ecosystems (Fang et al., 2015; Russell and Raich, 2012; Tietema and Verstraten,
878 1991; Bai et al., 2012) (Table 4). We fully acknowledge that this simple approach is not as
879 robust as bottom-up, process-based emissions inventories (Werner et al., 2007). Even so, we
880 believe it is still useful for providing first-order approximations of annual N_2O , N_2 and total
881 gaseous N flux.

882

883 To briefly summarize our methodology, our first step was to use published surface area
884 estimates for the different habitats in the Kosñipata Valley to derive areal fractions for each
885 habitat (Feeley and Silman, 2010) (Table 4). Next, we multiplied the unweighted seasonal
886 mean flux by the areal fraction for each habitat to derive area-weighted seasonal flux
887 estimates (Table 4). We subsequently multiplied the area-weighted seasonal flux by the
888 fraction of the year accounted for by either season, in order to produce an area-weighted
889 and seasonally-weighted annual flux estimate for each habitat (Table 4). The final step of this
890 process was to sum the area-weighted and seasonally-weighted flux estimates for each
891 habitat, to drive an overall weighted flux estimate for the Kosñipata Valley as a whole (Table
892 4). Weighted annual estimates of N_2 flux were calculated using the N_2O yield values for each
893 habitat as determined in our soil moisture manipulation experiment (Table 4). We elected to
894 use mean N_2O yields for each habitat, rather than estimating N_2O yield based on soil
895 moisture content, because ANCOVA indicated that habitat was a better predictor of N_2O
896 yield than soil moisture, explaining a substantially greater proportion of the variance (i.e. 10
897 % versus only 1 % of the variance; see Supplementary Online Materials Table S2C). Total
898 gaseous N export was estimate by calculating the sum of annual N_2O and N_2 flux. Errors for
899 all the annual flux estimates (i.e. N_2O , N_2 , total gaseous N) were propagated using standard
900 error propagation techniques.

901

902 We determined that the Kosñipata Valley emitted approximately $1.27 \pm 0.33 \text{ kg N}_2\text{O-N ha}^{-1}$
903 year^{-1} , $3.29 \pm 1.27 \text{ kg N}_2\text{-N ha}^{-1} \text{ year}^{-1}$, and $4.57 \pm 1.31 \text{ kg N ha}^{-1} \text{ year}^{-1}$. Annual N_2O flux was
904 broadly on par with our earlier estimates (i.e. $1.18 \pm 0.79 \text{ kg N}_2\text{O-N ha}^{-1} \text{ year}^{-1}$) (Teh et al.,
905 2014). This estimated annual rate of flux exceeds the value for montane tropical montane
906 forests calculated by Werner et al. (2007) using a bottom-up process model (i.e. 0.5 to 1 kg
907 $\text{N}_2\text{O-N ha}^{-1} \text{ year}^{-1}$), but falls within the range predicted for humid tropical forest soils more
908 generally (i.e. approximately 1-4 kg $\text{N}_2\text{O-N ha}^{-1} \text{ year}^{-1}$) (van Lent et al., 2015; Werner et al.,
909 2007). Annual N_2 flux and total gaseous N flux are at the lower end of the range reported in
910 comparable studies from other ecosystems (e.g. Fang et al., 2015 reported annual gaseous
911 losses of 5.6– 30.1 kg N $\text{ha}^{-1} \text{ year}^{-1}$ sampling across a broad range of temperate and tropical
912 ecosystems) (Fang et al., 2015; Russell and Raich, 2012; Tietema and Verstraten, 1991; Bai et
913 al., 2012), further supporting claims that Andean ecosystems are relatively N limited, and
914 may cycle N more conservatively than lowland forests (Baldos et al., 2015; Müller et al.,
915 2015; Wolf et al., 2011; Nottingham et al., 2015)

916

917

918 **7. Conclusions**

919 Process-based studies of N_2O flux from montane tropical ecosystems in the southern
920 Peruvian Andes affirms prior research suggesting that these ecosystems are potentially
921 important regional sources of N_2O (Teh et al., 2014). Simple weighted upscaling suggests
922 that annual N_2O flux from the Kosñipata Valley is on the order of $1.27 \pm 0.33 \text{ kg N}_2\text{O-N ha}^{-1}$.
923 Habitat – a proxy for NO_3^- availability under field conditions – was the best predictor for N_2O
924 flux, with more N-rich habitats (i.e. premontane forest) showing significantly higher N_2O flux
925 than habitats with lower N availability (i.e. upper montane forest, montane grassland).
926 Nitrous oxide flux originated primarily from nitrate reduction rather than from nitrification,
927 probably due to low pH soil conditions which may have inhibited the activity of AOB.
928 Contrary to our prior research, we found only weak evidence for seasonal trends in field N_2O
929 flux, with the exception of lower montane forest, which showed significantly higher N_2O flux
930 during the dry season compared to the wet season. Weak seasonal trends in field N_2O flux
931 among the other montane habitats probably stems from relatively modest seasonal
932 variation in key environmental drivers (e.g. temperature, WFPS, NO_3^-), combined with a soil

933 moisture response that was complex and non-linear. Nitrous oxide flux was significantly
934 influenced by soil moisture content, but the trends in N₂O production and flux diverged from
935 theoretical norms. For example, we saw little evidence of N₂O production from ammonia-
936 oxidation, even though the field measurement (i.e. resin bags) indicate that nitrification
937 occurs. This may be due to the predominance of AOA, which produce significantly N₂O than
938 AOB, under the acidic conditions common in Andean soils. At higher soil moisture levels, N₂O
939 flux increased non-linearly with WFPS, with peaks in N₂O flux at 90 and 50 % WFPS. These
940 results suggest that the effects of water on N₂O flux are complicated by other factors, such
941 as competition for substrates among different nitrate-reducing processes, or shifts in the
942 amount of N₂O derived from denitrification or DNRA. Field data and substrate manipulation
943 experiments indicated that N₂O flux was strongly limited by NO₃⁻, but unconstrained by the
944 input rate of labile organic matter (i.e. leaf litter). Nitrous oxide flux was relatively insensitive
945 to short-term variations in NO₃⁻, and was better-predicted by longer-term, time-averaged
946 variations in NO₃⁻ availability.

947

948

949 **8. Data Availability**

950 Data for this publication are publically available from the UK Natural Environment Research
951 Council (NERC) Centre for Environmental Data Analysis (CEDA), at the following URL:

952 <http://catalogue.ceda.ac.uk/uuid/93fdb48b713b4dbc93a28d695771312d>

953

954

955 **9. Author Contributions**

956 TD designed the field and laboratory experiments, collected the field data, conducted the
957 laboratory experiments, processed the samples, analysed the data, and contributed to the
958 preparation of the manuscript. NJM contributed to the design of the laboratory
959 experiments, assisted in the sample analysis, assisted in the analysis of the laboratory data,
960 and contributed to the preparation of the manuscript. AJC and LPHQ assisted in the
961 collection of the field data and processing of the field samples. EMB, PM, MR, and PS
962 contributed to the experimental design and the preparation of the manuscript. YAT directed
963 the research, contributed to the design of the experiments, assisted in the analysis of the
964 field and laboratory data, and took the principal role in preparing the manuscript.

965

966

967 **10. Acknowledgements**

968 The authors would like to acknowledge the agencies that funded this research; the UK
969 Natural Environment Research Council (NERC; joint grant references NE/H006583,
970 NE/H007849 and NE/H006753). Patrick Meir was supported by an Australian Research
971 Council Fellowship (FT110100457). Javier Eduardo Silva Espejo, Walter Huaraca Huasco, and
972 the ABIDA NGO provided critical fieldwork and logistical support. Angus Calder (University of
973 St Andrews) and Vicky Munro (University of Aberdeen) provided invaluable laboratory
974 support. Thanks to Adrian Tejedor from the Amazon Conservation Association, who provided
975 assistance with site access and site selection at Hacienda Villa Carmen. This publication is a
976 contribution from the Scottish Alliance for Geoscience, Environment and Society
977 (<http://www.sages.ac.uk>).

978

979

980 **11. References**

981 Baggs, E. M., Richter, M., Hartwig, U.A., and Cadisch, G. : Nitrous oxide emissions from grass
982 swards during the eighth year of elevated atmospheric pCO₂ (Swiss FACE). , *Global Change*
983 *Biology* 9, 1214-1222., 2003.

984 Bai, E., Houlton, B. Z., and Wang, Y. P.: Isotopic identification of nitrogen hotspots across
985 natural terrestrial ecosystems, *Biogeosciences*, 9, 3287-3304, 10.5194/bg-9-3287-2012,
986 2012.

987 Baldos, A. P., Corre, M. D., and Veldkamp, E.: Response of N cycling to nutrient inputs in
988 forest soils across a 1000–3000 m elevation gradient in the Ecuadorian Andes, *Ecology*, 96,
989 749-761, 10.1890/14-0295.1, 2015.

990 Bateman, E. J., and Baggs, E. M.: Contributions of nitrification and denitrification to N₂O
991 emissions from soils at different water-filled pore space, *Biology and Fertility of Soils*, 41,
992 379-388, 10.1007/s00374-005-0858-3, 2005.

993 Belyea, L. R., and Baird, A. J.: Beyond "The limits to peat bog growth": Cross-scale feedback
994 in peatland development, *Ecological Monographs*, 76, 299-322, 2006.

995 Blackmer, A. M., and Bremner, J. M.: Inhibitory effect of nitrate on reduction of N₂O to N₂
996 by soil microorganisms, *Soil Biology and Biochemistry*, 10, 187-191,
997 [http://dx.doi.org/10.1016/0038-0717\(78\)90095-0](http://dx.doi.org/10.1016/0038-0717(78)90095-0), 1978.
998 Breuer, L., Papen, H., and Butterbach-Bahl, K.: N₂O emission from tropical forest soils of
999 Australia, *J. Geophys. Res.-Atmos.*, 105, 26353-26367, 10.1029/2000jd900424, 2000.
1000 Corre, M. D., Veldkamp, E., Arnold, J., and Wright, S. J.: Impact of elevated N input on soil N
1001 cycling and losses in old-growth lowland and montane forests in Panama, *Ecology*, 91, 1715-
1002 1729, 10.1890/09-0274.1, 2010.
1003 Davidson, E. A.: Fluxes of nitrous oxide and nitric oxide from terrestrial ecosystems, in:
1004 Microbial production and consumption of greenhouse gases: methane, nitrogen oxides, and
1005 halomethanes., edited by: Rogers, J. E., and Whitman, W. B., American Society for
1006 Microbiology, Washington D.C., 219-236, 1991.
1007 Davidson, E. A., and Verchot, L. V.: Testing the Hole-in-the-Pipe Model of nitric and nitrous
1008 oxide emissions from soils using the TRAGNET Database, *Global Biogeochemical Cycles*, 14,
1009 1035-1043, 10.1029/1999GB001223, 2000.
1010 Eva, H. D., Belward, A. S., De Miranda, E. E., Di Bella, C. M., Gond, V., Huber, O., Jones, S.,
1011 Sgrenzaroli, M., and Fritz, S.: A land cover map of South America, *Global Change Biology*, 10,
1012 731-744, 10.1111/j.1529-8817.2003.00774.x, 2004.
1013 Fang, Y., Koba, K., Makabe, A., Takahashi, C., Zhu, W., Hayashi, T., Hokari, A. A., Urakawa, R.,
1014 Bai, E., Houlton, B. Z., Xi, D., Zhang, S., Matsushita, K., Tu, Y., Liu, D., Zhu, F., Wang, Z., Zhou,
1015 G., Chen, D., Makita, T., Toda, H., Liu, X., Chen, Q., Zhang, D., Li, Y., and Yoh, M.: Microbial
1016 denitrification dominates nitrate losses from forest ecosystems, *Proceedings of the National*
1017 *Academy of Sciences*, 112, 1470-1474, 10.1073/pnas.1416776112, 2015.
1018 Feeley, K. J., and Silman, M. R.: Land-use and climate change effects on population size and
1019 extinction risk of Andean plants, *Global Change Biology*, 16, 3215-3222, 10.1111/j.1365-
1020 2486.2010.02197.x, 2010.
1021 Firestone, M. K., Firestone, R. B., and Tiedge, J. M.: Nitrous oxide from soil denitrification:
1022 Factors controlling its biological production., *Science*, 208, 749-751, 1980.
1023 Firestone, M. K., and Davidson, E. A.: Microbiological basis of NO and N₂O production and
1024 consumption in soil, in: *Exchange of Trace Gases Between Terrestrial Ecosystems and the*
1025 *Atmosphere*, edited by: Andrae, M. O., and Schimel, D. S., John Wiley and Sons Ltd., New
1026 York, 7-21, 1989.

1027 Girardin, C. A. J., Malhi, Y., Aragão, L. E. O. C., Mamani, M., Huaraca Huasco, W., Durand, L.,
1028 Feeley, K. J., Rapp, J., Silva-Espejo, J. E., Silman, M., Salinas, N., and Whittaker, R. J.: Net
1029 primary productivity allocation and cycling of carbon along a tropical forest elevational
1030 transect in the Peruvian Andes, *Global Change Biology*, 16, 3176-3192, 10.1111/j.1365-
1031 2486.2010.02235.x, 2010.

1032 Groffman, P. M., Butterbach-Bahl, K., Fulweiler, R. W., Gold, A. J., Morse, J. L., Stander, E. K.,
1033 Tague, C., Tonitto, C., and Vidon, P.: Challenges to incorporating spatially and temporally
1034 explicit phenomena (hotspots and hot moments) in denitrification models, *Biogeochemistry*,
1035 93, 49-77, 10.1007/s10533-008-9277-5, 2009.

1036 Hall, S. J., and Matson, P. A.: Nitrogen oxide emissions after nitrogen additions in tropical
1037 forests, *Nature*, 400, 152-155, 1999.

1038 Hink, L., Nicol, G. W., and Prosser, J. I.: Archaea produce lower yields of N₂O than bacteria
1039 during aerobic ammonia oxidation in soil, *Environ. Microbiol.*, n/a-n/a, 10.1111/1462-
1040 2920.13282, 2016.

1041 Hirsch, A. I., Michalak, A. M., Bruhwiler, L. M., Peters, W., Dlugokencky, E. J., and Tans, P. P.:
1042 Inverse modeling estimates of the global nitrous oxide surface flux from 1998-2001, *Global
1043 Biogeochemical Cycles*, 20, 1-17, Gb1008
1044 10.1029/2004gb002443, 2006.

1045 Holtan-Hartwig, L., Dorsch, P., and Bakken, L. R.: Comparison of denitrifying communities in
1046 organic soils: kinetics of NO₃⁻ and N₂O reduction, *Soil Biol. Biochem.*, 32, 833-843,
1047 10.1016/s0038-0717(99)00213-8, 2000.

1048 Huang, J., Golombek, A., Prinn, R., Weiss, R., Fraser, P., Simmonds, P., Dlugokencky, E. J.,
1049 Hall, B., Elkins, J., Steele, P., Langenfelds, R., Krummel, P., Dutton, G., and Porter, L.:
1050 Estimation of regional emissions of nitrous oxide from 1997 to 2005 using multinetwork
1051 measurements, a chemical transport model, and an inverse method, *J. Geophys. Res.-
1052 Atmos.*, 113, 1-19, D17313
1053 10.1029/2007jd009381, 2008.

1054 Jones, S. P., Diem, T., Huaraca Quispe, L. P., Cahuana, A. J., Reay, D. S., Meir, P., and Teh, Y.
1055 A.: Drivers of atmospheric methane uptake by montane forest soils in the southern Peruvian
1056 Andes, *Biogeosciences*, 13, 4151-4165, 10.5194/bg-13-4151-2016, 2016.

1057 Koehler, B., Corre, M. D., Steger, K., Well, R., Zehe, E., Sueta, J. P., and Veldkamp, E.: An in-
1058 depth look into a tropical lowland forest soil: nitrogen-addition effects on the contents of

1059 N₂O, CO₂ and CH₄ and N₂O isotopic signatures down to 2-m depth, *Biogeochemistry*, 111,
1060 695-713, 10.1007/s10533-012-9711-6, 2012.

1061 Kort, E. A., Patra, P. K., Ishijima, K., Daube, B. C., Jimenez, R., Elkins, J., Hurst, D., Moore, F. L.,
1062 Sweeney, C., and Wofsy, S. C.: Tropospheric distribution and variability of N₂O: Evidence for
1063 strong tropical emissions, *Geophys. Res. Lett.*, 38, 5, 10.1029/2011gl047612, 2011.

1064 Li, C., Aber, J., Stange, F., Butterbach-Bahl, K., and Papen, H.: A process-oriented model of
1065 N₂O and NO emissions from forest soils: 1. Model development, *Journal of Geophysical*
1066 *Research: Atmospheres*, 105, 4369-4384, 10.1029/1999JD900949, 2000.

1067 Limmer, A. W., and Steele, K. W.: Denitrification potentials: Measurement of seasonal
1068 variation using a short-term anaerobic incubation technique, *Soil Biology and Biochemistry*,
1069 14, 179-184, [http://dx.doi.org/10.1016/0038-0717\(82\)90020-7](http://dx.doi.org/10.1016/0038-0717(82)90020-7), 1982.

1070 Livingston, G., and Hutchinson, G.: Chapter 2: Enclosure-based measurement of trace gas
1071 exchange: applications and sources of error., in: *Biogenic Trace Gases: Measuring Emissions*
1072 *from Soil and Water.*, edited by: Matson, P., Harriss, RC, Blackwell Science Ltd, Cambridge,
1073 MA, USA, 14-51, 1995.

1074 Malhi, Y., Silman, M., Salinas, N., Bush, M., Meir, P., and Saatchi, S.: Introduction: Elevation
1075 gradients in the tropics: laboratories for ecosystem ecology and global change research,
1076 *Global Change Biology*, 16, 3171-3175, 10.1111/j.1365-2486.2010.02323.x, 2010.

1077 Morley, N., and Baggs, E. M.: Carbon and oxygen controls on N₂O and N₂ production during
1078 nitrate reduction, *Soil Biol. Biochem.*, 42, 1864-1871, 10.1016/j.soilbio.2010.07.008, 2010.

1079 Moser, G., Leuschner, C., Hertel, D., Graefe, S., Soethe, N., and Iost, S.: Elevation effects on
1080 the carbon budget of tropical mountain forests (S Ecuador): the role of the belowground
1081 compartment, *Global Change Biology*, 17, 2211-2226, 10.1111/j.1365-2486.2010.02367.x,
1082 2011.

1083 Müller, A. K., Matson, A. L., Corre, M. D., and Veldkamp, E.: Soil N₂O fluxes along an
1084 elevation gradient of tropical montane forests under experimental nitrogen and phosphorus
1085 addition, *Frontiers in Earth Science*, 3, 66, 2015.

1086 Nevison, C. D., Lueker, T. J., and Weiss, R. F.: Quantifying the nitrous oxide source from
1087 coastal upwelling, *Global Biogeochemical Cycles*, 18, 24, Gb1018
1088 10.1029/2003gb002110, 2004.

1089 Nevison, C. D., Mahowald, N. M., Weiss, R. F., and Prinn, R. G.: Interannual and seasonal
1090 variability in atmospheric N₂O, *Global Biogeochemical Cycles*, 21, GB3017,
1091 10.1029/2006GB002755, 2007.

1092 Nottingham, A. T., Turner, B. L., Whitaker, J., Ostle, N. J., McNamara, N. P., Bardgett, R. D.,
1093 Salinas, N., and Meir, P.: Soil microbial nutrient constraints along a tropical forest elevation
1094 gradient: a belowground test of a biogeochemical paradigm, *Biogeosciences*, 12, 6071-6083,
1095 10.5194/bg-12-6071-2015, 2015.

1096 Parton, W. J., Mosier, A. R., Ojima, D. S., Valentine, D. W., Schimel, D. S., Weier, K., and
1097 Kulmala, A. E.: Generalized model for N₂ and N₂O production from nitrification and
1098 denitrification, *Global Biogeochemical Cycles*, 10, 401-412, 10.1029/96GB01455, 1996.

1099 Pedersen, A. R., Petersen, S. O., and Schelde, K.: A comprehensive approach to soil-
1100 atmosphere trace-gas flux estimation with static chambers, *European Journal of Soil Science*,
1101 61, 888-902, 10.1111/j.1365-2389.2010.01291.x, 2010.

1102 Pett-Ridge, J., and Firestone, M. K.: Redox fluctuation structures microbial communities in a
1103 wet tropical soil, *Appl. Environ. Microbiol.*, 71, 6998-7007, 10.1128/aem.71.11.6998-
1104 7007.2005, 2005.

1105 Potter, C. S., Matson, P. A., Vitousek, P. M., and Davidson, E. A.: Process modeling of controls
1106 on nitrogen trace gas emissions from soils worldwide, *Journal of Geophysical Research:*
1107 *Atmospheres*, 101, 1361-1377, 10.1029/95JD02028, 1996.

1108 Prosser, J. I., and Nicol, G. W.: Relative contributions of archaea and bacteria to aerobic
1109 ammonia oxidation in the environment, *Environ. Microbiol.*, 10, 2931-2941, 10.1111/j.1462-
1110 2920.2008.01775.x, 2008.

1111 Pumpanen, J., Kolari, P., Ilvesniemi, H., Minkkinen, K., Vesala, T., Niinistö, S., Lohila, A.,
1112 Larmola, T., Morero, M., Pihlatie, M., Janssens, I., Yuste, J. C., Grünzweig, J. M., Reth, S.,
1113 Subke, J.-A., Savage, K., Kutsch, W., Østreg, G., Ziegler, W., Anthoni, P., Lindroth, A., and
1114 Hari, P.: Comparison of different chamber techniques for measuring soil CO₂ efflux, *Agric.*
1115 *For. Meteorol.*, 123, 159-176, <http://dx.doi.org/10.1016/j.agrformet.2003.12.001>, 2004.

1116 Russell, A. E., and Raich, J. W.: Rapidly growing tropical trees mobilize remarkable amounts
1117 of nitrogen, in ways that differ surprisingly among species, *Proceedings of the National*
1118 *Academy of Sciences*, 109, 10398-10402, 10.1073/pnas.1204157109, 2012.

1119 Saikawa, E., Schlosser, C. A., and Prinn, R. G.: Global modeling of soil nitrous oxide emissions
1120 from natural processes, *Global Biogeochemical Cycles*, 27, 972-989, 10.1002/gbc.20087,
1121 2013.

1122 Saikawa, E., Prinn, R. G., Dlugokencky, E., Ishijima, K., Dutton, G. S., Hall, B. D., Langenfelds,
1123 R., Tohjima, Y., Machida, T., Manizza, M., Rigby, M., O'Doherty, S., Patra, P. K., Harth, C. M.,
1124 Weiss, R. F., Krummel, P. B., van der Schoot, M., Fraser, P. J., Steele, L. P., Aoki, S., Nakazawa,
1125 T., and Elkins, J. W.: Global and regional emissions estimates for N₂O, *Atmospheric*
1126 *Chemistry and Physics*, 14, 4617-4641, 10.5194/acp-14-4617-2014, 2014.

1127 Schlesinger, W. H.: On the fate of anthropogenic nitrogen, *Proceedings of the National*
1128 *Academy of Sciences*, 106, 203-208, 10.1073/pnas.0810193105, 2009.

1129 Silver, W. L., Herman, D. J., and Firestone, M. K. S.: Dissimilatory Nitrate Reduction to
1130 Ammonium in Upland Tropical Forest Soils., *Ecology*, 82, 2410-2416, 2001.

1131 Smith, P., Smith, J. U., Flynn, H., Killham, K., Rangel-Castro, I., Foereid, B., Aitkenhead, M.,
1132 Chapman, S., Towers, W., Bell, J., Lumsdon, D., Milne, R., Thomson, A., Simmons, I., Skiba, U.,
1133 Reynolds, B., Evans, C., Frogbrook, Z., Bradley, I., Whitmore, A., and Falloon, P.: ECOSSE:
1134 Estimating Carbon in Organic Soils - Sequestration and Emissions. Final Report., Scottish
1135 Executive Environment and Rural Affairs Department Report, 166 pp., 2007.

1136 Streminska, M. A., Felgate, H., Rowley, G., Richardson, D. J., and Baggs, E. M.: Nitrous oxide
1137 production in soil isolates of nitrate-ammonifying bacteria, *Environ. Microbiol. Rep.*, 4, 66-
1138 71, 10.1111/j.1758-2229.2011.00302.x, 2012.

1139 Subler, S., Blair, J. M., and Edwards, C. A.: Using anion-exchange membranes to measure soil
1140 nitrate availability and net nitrification, *Soil Biology and Biochemistry*, 27, 911-917,
1141 [http://dx.doi.org/10.1016/0038-0717\(95\)00008-3](http://dx.doi.org/10.1016/0038-0717(95)00008-3), 1995.

1142 Team, R. C.: A language and environment for statistical computing, R Foundation for
1143 Statistical Computing, Vienna, Austria, 2012.

1144 Teh, Y. A., Diem, T., Jones, S., Huaraca Quispe, L. P., Baggs, E., Morley, N., Richards, M.,
1145 Smith, P., and Meir, P.: Methane and nitrous oxide fluxes across an elevation gradient in the
1146 tropical Peruvian Andes, *Biogeosciences*, 11, 2325-2339, 10.5194/bg-11-2325-2014, 2014.

1147 Templer, P. H., Lovett, G. M., Weathers, K. C., Findlay, S. E., and Dawson, T. E.: Influence of
1148 tree species on forest nitrogen retention in the Catskill Mountains, New York, USA,
1149 *Ecosystems*, 8, 1-16, 10.1007/s10021-004-0230-8, 2005.

1150 Tietema, A., and Verstraten, J. M.: Nitrogen cycling in an acid forest ecosystem in the
1151 Netherlands under increased atmospheric nitrogen input, *Biogeochemistry*, 15, 21-46,
1152 10.1007/bf00002807, 1991.

1153 van Lent, J., Hergoualc'h, K., and Verchot, L. V.: Reviews and syntheses: Soil N₂O and NO
1154 emissions from land use and land use change in the tropics and subtropics: a meta-analysis,
1155 *Biogeosciences*, 15, 7299-7313 pp., 2015.

1156 Varner, R. K., Keller, M., Robertson, J. R., Dias, J. D., Silva, H., Crill, P. M., McGroddy, M., and
1157 Silver, W. L.: Experimentally induced root mortality increased nitrous oxide emission from
1158 tropical forest soils, *Geophys. Res. Lett.*, 30, n/a-n/a, 10.1029/2002GL016164, 2003.

1159 Veldkamp, E., Purbopuspito, J., Corre, M. D., Brumme, R., and Murdiyarso, D.: Land use
1160 change effects on trace gas fluxes in the forest margins of Central Sulawesi, Indonesia,
1161 *Journal of Geophysical Research-Biogeosciences*, 113, 1-11, G02003
1162 10.1029/2007jg000522, 2008.

1163 Weier, K. L., Doran, J. W., Power, J. F., and Walters, D. T.: Denitrification and the denitrogen
1164 nitrous oxide ratio as affected by soil water, available carbon, and nitrate, *Soil Sci. Soc. Am.*
1165 *J.*, 57, 66-72, 1993.

1166 Werner, C., Butterbach-Bahl, K., Haas, E., Hickler, T., and Kiese, R.: A global inventory of N₂O
1167 emissions from tropical rainforest soils using a detailed biogeochemical model, *Global*
1168 *Biogeochemical Cycles*, 21, 1-18, Gb3010
1169 10.1029/2006gb002909, 2007.

1170 Wolf, K., Veldkamp, E., Homeier, J., and Martinson, G. O.: Nitrogen availability links forest
1171 productivity, soil nitrous oxide and nitric oxide fluxes of a tropical montane forest in
1172 southern Ecuador, *Global Biogeochemical Cycles*, 25, GB4009, 10.1029/2010GB003876,
1173 2011.

1174 Wolf, K., Flessa, H., and Veldkamp, E.: Atmospheric methane uptake by tropical montane
1175 forest soils and the contribution of organic layers, *Biogeochemistry*, 111, 469-483,
1176 10.1007/s10533-011-9681-0, 2012.

1177 Zimmermann, M., Meir, P., Bird, M., Malhi, Y., and Ccahuana, A.: Litter contribution to
1178 diurnal and annual soil respiration in a tropical montane cloud forest, *Soil Biology and*
1179 *Biochemistry*, 41, 1338-1340, 2009a.

1180 Zimmermann, M., Meir, P., Bird, M. I., Malhi, Y., and Ccahuana, A. J. Q.: Climate dependence
1181 of heterotrophic soil respiration from a soil-translocation experiment along a 3000 m

1182 tropical forest altitudinal gradient, *European Journal of Soil Science*, 60, 895-906,
1183 10.1111/j.1365-2389.2009.01175.x, 2009b.
1184 Zimmermann, M., Leifeld, J., Conen, F., Bird, M. I., and Meir, P.: Can composition and
1185 physical protection of soil organic matter explain soil respiration temperature sensitivity?,
1186 *Biogeochemistry*, 107, 423-436, 10.1007/s10533-010-9562-y, 2012.
1187
1188

Elevation Band m a.s.l.	Habitat	Latitude	Longitude	Mean Annual Temperature °C	Mean Annual Precipitation mm	Bulk density 0-10 cm g/cm ³	pH	Soil CN 0-10 cm	Soil C 0-10 cm %	0-10 cm			10-30 cm			Landforms	Plots n	Flux Chambers n
										Clay	Silt	Sand	Clay	Silt	Sand			
600-1200	Premontane forest	12°53'43"	71°23'04"	20.5	5318	0.38 ± 0.03 (n = 21)	3.4 ± 0.1	11.3 ± 0.2	7.9 ± 0.5	5.4 ± 0.3	68.8 ± 3.9	25.4 ± 15.9	8.9 ± 1.8	81.0 ± 1.7	10.3 ± 2.5	ridge, slope, flat	3	15
1200-2200	Lower montane forest	13°25'56"	71°32'13"	17.2	2631	0.19 ± 0.03 (n = 17)	3.4 ± 0.1	14.5 ± 0.2	25.2 ± 1.3	3.6 ± 0.4	67.3 ± 4.2	29.3 ± 4.5	7.2 ± 0.4	83.8 ± 0.8	9.0 ± 0.9	ridge, slope, flat	3	15
2200-3200	Upper montane forest	13°11'24"	71°35'13"	10.7	1706	0.41 ± 0.02 (n = 12)	3.9 ± 0.1	16.8 ± 0.4	16.3 ± 1.0	5.1 ± 0.9	57.1 ± 7.9	37.9 ± 8.7	4.4 ± 2.0	46.5 ± 1.62	49.1 ± 1.81	ridge, slope	3	15
3200-3700	Montane grassland	13°07'19"	71°36'54"	9.3	2200	0.36 ± 0.03 (n = 27)	4.1 ± 0.1	12.9 ± 0.4	16.0 ± 1.0	2.6 ± 0.2	54.4 ± 3.0	43.0 ± 3.2	n/a	n/a	n/a	ridge, slope, flat, basin	4	20

1192 **Table 2.** Description of the water-filled pore space and NO₃⁻ addition treatments for the
 1193 laboratory manipulation experiments.

Habitat	Experimental Treatment	Soil Depth	Soil Type	WFPS %	Inorganic N added ng N (g soil) ⁻¹	¹⁵ N Tracer	Replicate n
WATER-FILLED PORE SPACE							
Premontane forest	90 % WFPS	0-10	mineral	90	200	¹⁵ NH ₄ ⁺ ¹⁵ NO ₃ ⁻	5
	90 % WFPS	0-10	mineral	90	200	¹⁴ NH ₄ ⁺ ¹⁵ NO ₃ ⁻	5
	70 % WFPS	0-10	mineral	70	200	¹⁵ NH ₄ ⁺ ¹⁵ NO ₃ ⁻	5
	70 % WFPS	0-10	mineral	70	200	¹⁴ NH ₄ ⁺ ¹⁵ NO ₃ ⁻	5
	50 % WFPS	0-10	mineral	50	200	¹⁵ NH ₄ ⁺ ¹⁵ NO ₃ ⁻	5
	50 % WFPS	0-10	mineral	50	200	¹⁴ NH ₄ ⁺ ¹⁵ NO ₃ ⁻	5
Lower montane forest	30 % WFPS	0-10	mineral	30	200	¹⁵ NH ₄ ⁺ ¹⁵ NO ₃ ⁻	5
	30 % WFPS	0-10	mineral	30	200	¹⁴ NH ₄ ⁺ ¹⁵ NO ₃ ⁻	5
	90 % WFPS	0-10	mineral	90	200	¹⁵ NH ₄ ⁺ ¹⁵ NO ₃ ⁻	5
	90 % WFPS	0-10	mineral	90	200	¹⁴ NH ₄ ⁺ ¹⁵ NO ₃ ⁻	5
	70 % WFPS	0-10	mineral	70	200	¹⁵ NH ₄ ⁺ ¹⁵ NO ₃ ⁻	5
	70 % WFPS	0-10	mineral	70	200	¹⁴ NH ₄ ⁺ ¹⁵ NO ₃ ⁻	5
Upper montane forest	50 % WFPS	0-10	mineral	50	200	¹⁵ NH ₄ ⁺ ¹⁵ NO ₃ ⁻	5
	50 % WFPS	0-10	mineral	50	200	¹⁴ NH ₄ ⁺ ¹⁵ NO ₃ ⁻	5
	30 % WFPS	0-10	mineral	30	200	¹⁵ NH ₄ ⁺ ¹⁵ NO ₃ ⁻	5
	30 % WFPS	0-10	mineral	30	200	¹⁴ NH ₄ ⁺ ¹⁵ NO ₃ ⁻	5
	90 % WFPS	10-20	mineral	90	20	¹⁵ NH ₄ ⁺ ¹⁵ NO ₃ ⁻	5
	90 % WFPS	10-20	mineral	90	20	¹⁴ NH ₄ ⁺ ¹⁵ NO ₃ ⁻	5
Montane grassland	70 % WFPS	10-20	mineral	70	20	¹⁵ NH ₄ ⁺ ¹⁵ NO ₃ ⁻	5
	70 % WFPS	10-20	mineral	70	20	¹⁴ NH ₄ ⁺ ¹⁵ NO ₃ ⁻	5
	50 % WFPS	10-20	mineral	50	20	¹⁵ NH ₄ ⁺ ¹⁵ NO ₃ ⁻	5
	50 % WFPS	10-20	mineral	50	20	¹⁴ NH ₄ ⁺ ¹⁵ NO ₃ ⁻	5
	30 % WFPS	10-20	mineral	30	20	¹⁵ NH ₄ ⁺ ¹⁵ NO ₃ ⁻	5
	30 % WFPS	10-20	mineral	30	20	¹⁴ NH ₄ ⁺ ¹⁵ NO ₃ ⁻	5
Premontane forest	control	0-10	mineral	80	n/a	n/a	5
	+50 % background NO ₃ ⁻	0-10	mineral	80	780 ± 60	K ¹⁵ NO ₃ ⁻	5
	+100 % background NO ₃ ⁻	0-10	mineral	80	1570 ± 120	K ¹⁵ NO ₃ ⁻	5
	+150 % background NO ₃ ⁻	0-10	mineral	80	2350 ± 170	K ¹⁵ NO ₃ ⁻	5
	control	0-10	mineral	80	n/a	n/a	5
	+50 % background NO ₃ ⁻	0-10	mineral	80	700 ± 60	K ¹⁵ NO ₃ ⁻	5
Lower montane forest	+100 % background NO ₃ ⁻	0-10	mineral	80	1400 ± 120	K ¹⁵ NO ₃ ⁻	5
	+150 % background NO ₃ ⁻	0-10	mineral	80	2100 ± 180	K ¹⁵ NO ₃ ⁻	5
	control	0-10	organic	80	n/a	n/a	5
	+50 % background NO ₃ ⁻	0-10	organic	80	90 ± 20	K ¹⁵ NO ₃ ⁻	5
	+100 % background NO ₃ ⁻	0-10	organic	80	180 ± 50	K ¹⁵ NO ₃ ⁻	5
	+150 % background NO ₃ ⁻	0-10	organic	80	270 ± 70	K ¹⁵ NO ₃ ⁻	5
Upper montane forest	control	10-20	mineral	80	n/a	n/a	5
	+50 % background NO ₃ ⁻	10-20	mineral	80	90 ± 40	K ¹⁵ NO ₃ ⁻	5
	+100 % background NO ₃ ⁻	10-20	mineral	80	190 ± 70	K ¹⁵ NO ₃ ⁻	5
	+150 % background NO ₃ ⁻	10-20	mineral	80	280 ± 110	K ¹⁵ NO ₃ ⁻	5
	control	0-10	mineral	80	n/a	n/a	5
	+50 % background NO ₃ ⁻	0-10	mineral	80	30 ± 10	K ¹⁵ NO ₃ ⁻	5
Montane grassland	+100 % background NO ₃ ⁻	0-10	mineral	80	60 ± 20	K ¹⁵ NO ₃ ⁻	5
	+150 % background NO ₃ ⁻	0-10	mineral	80	90 ± 40	K ¹⁵ NO ₃ ⁻	5

1194

1195 **Table 3.** Seasonal patterns in net N₂O flux, net inorganic N flux, and environmental variables.
 1196 Lower case letters indicate difference among seasons within habitats (*t*-Test on Box-Cox
 1197 transformed data, *P* < 0.05). Values reported here are means and standard errors.

Habitat	N ₂ O mg N-N ₂ O m ⁻² d ⁻¹		WFPS %		Soil Temperature °C		Air Temperature °C		Oxygen %		NO ₃ ⁻ µg N-NO ₃ ⁻ (g resin) ⁻¹ d ⁻¹		NH ₄ ⁺ µg N-NH ₄ ⁺ (g resin) ⁻¹ d ⁻¹	
	Wet Season	Dry Season	Wet Season	Dry Season	Wet Season	Dry Season	Wet Season	Dry Season	Wet Season	Dry Season	Wet Season	Dry Season	Wet Season	Dry Season
Premontane	0.71 ± 0.25 a n = 130	0.79 ± 0.26 a n = 98	51.9 ± 1.6 a n = 135	51.2 ± 2.1 a n = 135	20.7 ± 0.1 a n = 143	20.2 ± 0.1 b n = 120	21.5 ± 0.3 n = 143	20.4 ± 0.5 n = 120	19.4 ± 0.2 a n = 52	19.6 ± 0.2 a n = 36	22.2 ± 3.6 a n = 89	22.1 ± 2.1 a n = 96	31.4 ± 13.0 n = 90	11.3 ± 1.8 n = 95
Lower montane	0.09 ± 0.08 a n = 212	1.02 ± 0.58 b n = 137	42.2 ± 1.0 a n = 271	34.0 ± 1.4 b n = 179	18.1 ± 0.1 a n = 254	17.3 ± 0.2 b n = 164	18.9 ± 0.3 n = 254	18.3 ± 0.2 n = 164	19.2 ± 0.2 a n = 146	19.2 ± 0.1 a n = 81	11.8 ± 1.9 a n = 123	7.8 ± 1.4 a n = 94	20.2 ± 5.4 n = 124	8.6 ± 0.9 n = 93
Upper montane	0.06 ± 0.09 a n = 207	0.01 ± 0.11 a n = 146	42.0 ± 1.3 a n = 264	24.3 ± 1.4 b n = 180	11.8 ± 0.1 a n = 255	10.9 ± 0.2 b n = 165	12.8 ± 0.2 n = 255	12.5 ± 0.3 n = 165	18.7 ± 0.2 a n = 165	18.5 ± 0.2 a n = 109	1.4 ± 0.2 a n = 128	0.6 ± 0.2 b n = 91	22.5 ± 6.3 n = 129	11.3 ± 1.4 n = 93
Montane grassland	4.01 ± 0.11 a n = 238	0.19 ± 0.12 a n = 160	88.5 ± 0.3 a n = 303	88.3 ± 0.5 a n = 184	11.6 ± 0.1 a n = 282	9.0 ± 0.2 b n = 205	11.4 ± 0.3 n = 284	12.0 ± 0.5 n = 205	12.2 ± 0.9 a n = 176	15.4 ± 0.8 b n = 117	1.5 ± 0.4 a n = 128	2.1 ± 0.4 a n = 81	17.8 ± 4.3 n = 135	7.2 ± 0.8 n = 84

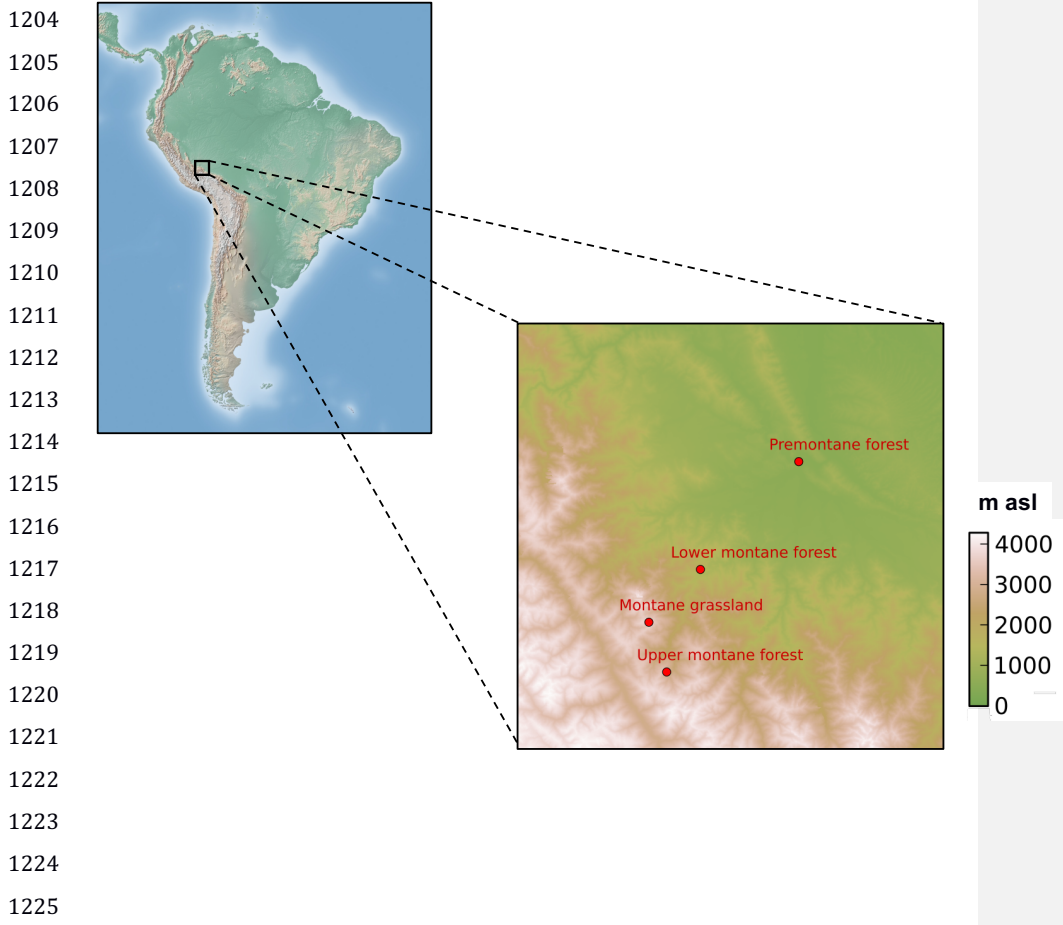
1198
1199

1200 **Table 4.** Area- and seasonally-weighted annual estimates of N₂O, N₂, and total gaseous N
 1201 flux

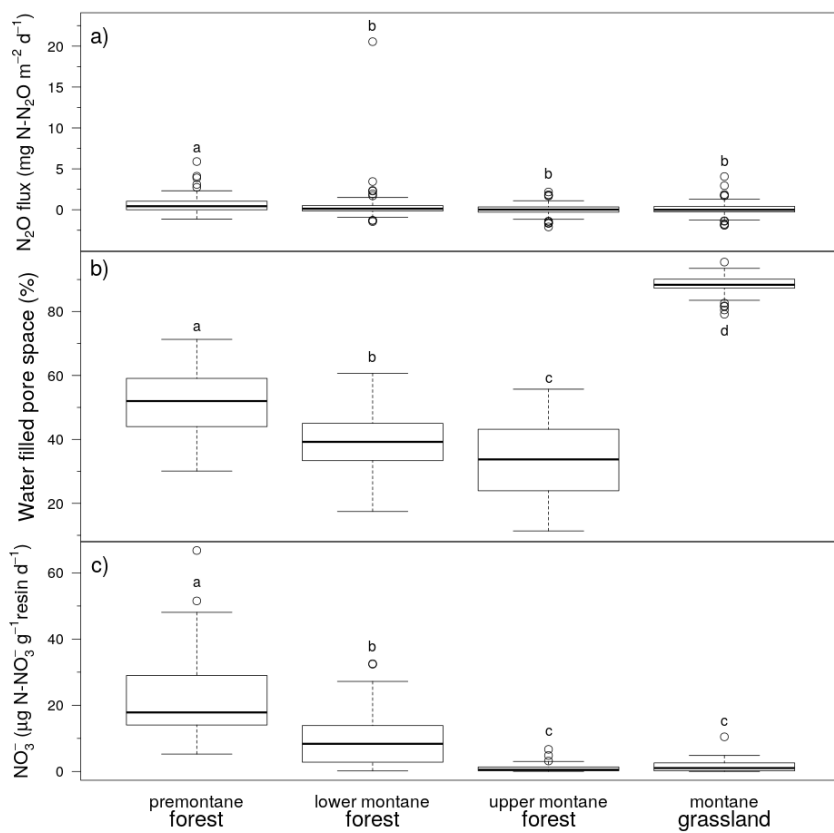
Elevation Band (m a.s.l.)	Habitat	Surface Area (ha)	Fraction of Land		Fraction of Year		Nitrous Oxide Yield		Unweighted Nitrous Oxide Flux		Area-weighted Nitrous Oxide Flux		Area-weighted and Seasonally-weighted Annual Estimate of N ₂ O Flux		Area-weighted and Seasonally-weighted Annual Estimate of N ₂ Flux		Area-weighted and Seasonally-weighted Annual Estimate of Total Gaseous N Flux		
			Area	Area	Wet Season	Dry Season	Wet Season	Dry Season	Wet Season	Dry Season	Wet Season	Dry Season	Wet Season	Dry Season	Wet Season	Dry Season	Wet Season	Dry Season	Wet Season
600-1200	Premontane forest	73000	0.24	0.58	0.42	0.42	0.41 ± 0.05	0.42	2.59 ± 0.91	2.88 ± 0.95	0.83 ± 0.22	0.70 ± 0.23	0.66 ± 0.16	1.09 ± 0.29	1.09 ± 0.29	1.61 ± 0.33	1.61 ± 0.33	1.61 ± 0.33	1.61 ± 0.33
1200-2200	Lower montane forest	82000	0.30	0.58	0.42	0.42	0.19 ± 0.04	0.42	0.31 ± 0.09	3.77 ± 1.12	0.10 ± 0.09	1.01 ± 0.63	0.21 ± 0.27	2.21 ± 1.24	2.21 ± 1.24	2.71 ± 1.26	2.71 ± 1.26	2.71 ± 1.26	2.71 ± 1.26
2200-3200	Upper montane forest	82000	0.27	0.58	0.42	0.42	0.42 ± 0.05	0.42	0.21 ± 0.13	0.04 ± 0.40	0.06 ± 0.09	0.51 ± 0.11	0.04 ± 0.07	0.05 ± 0.09	0.05 ± 0.09	0.09 ± 0.12	0.09 ± 0.12	0.09 ± 0.12	0.09 ± 0.12
3200-3700	Montane grasslands	58000	0.19	0.58	0.42	0.42	0.61 ± 0.06	0.42	-0.04 ± 0.60	0.09 ± 0.44	-0.01 ± 0.08	0.11 ± 0.09	0.05 ± 0.08	0.01 ± 0.04	0.01 ± 0.04	0.07 ± 0.07	0.07 ± 0.07	0.07 ± 0.07	0.07 ± 0.07
Total		302000											1.27 ± 0.33	3.29 ± 1.27	3.29 ± 1.27	4.57 ± 1.31	4.57 ± 1.31	4.57 ± 1.31	4.57 ± 1.31

1202

1203 **Figure 1.** Map of study sites across the Kosñipata Valley, Manu National Park, Peru.



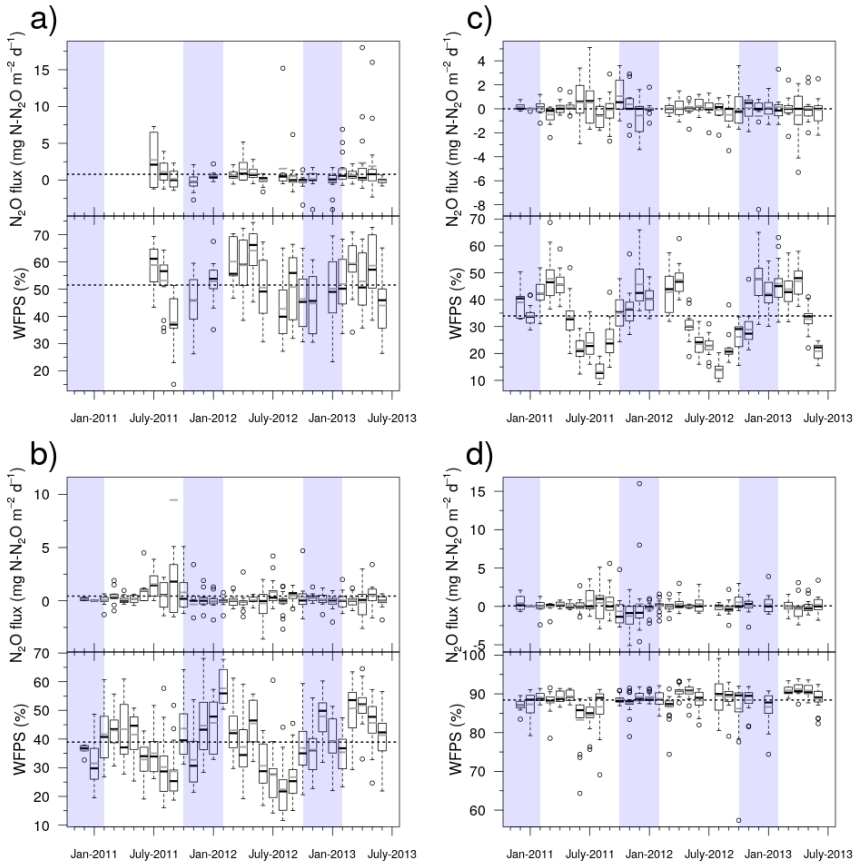
1226 **Figure 2.** Plot-averaged (a) net N₂O flux, (b) water-filled pore space, and (c) resin-extractable
1227 NO₃⁻ flux among habitats. Boxes enclose the interquartile range, whiskers indicate the 90th
1228 and 10th percentiles. Lower case letters indicate statistically significant differences among
1229 means (Fisher's LSD, *P* < 0.05).



1230
1231

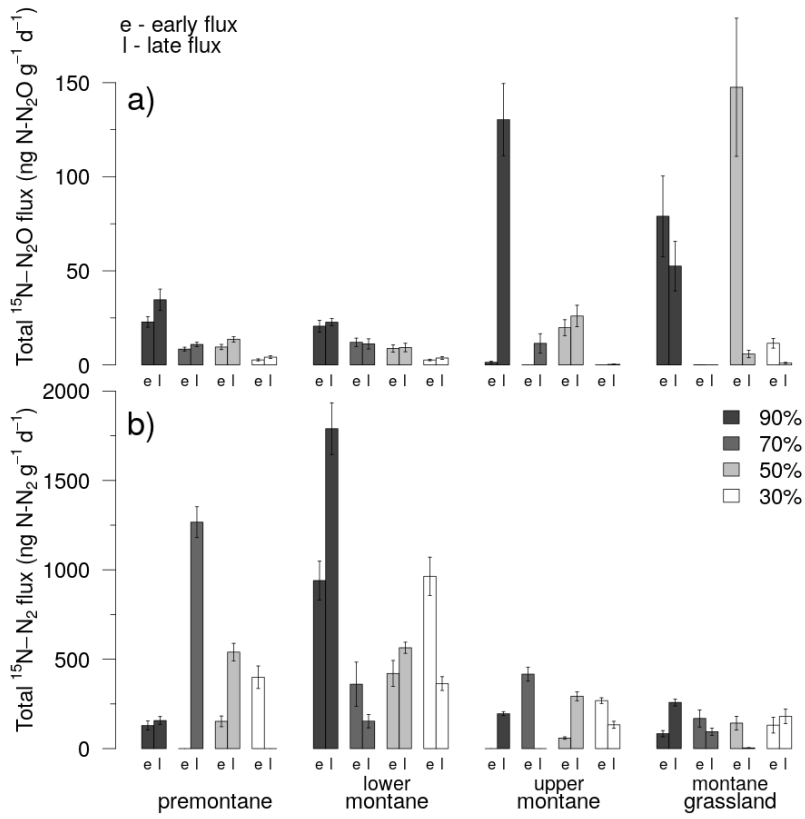
1232 **Figure 3.** Time series of net N₂O flux and water-filled pore space (WFPS). Panels indicate data
 1233 for (a) premontane forest, (b) lower montane forest, (c) upper montane forest, and (d)
 1234 montane grasslands for the 30-month study period beginning in January 2011 and ending in
 1235 June 2013. The broken horizontal line running across each panel denotes the overall mean
 1236 N₂O flux or WFPS for that habitat. The dashed line in each box indicate median values and
 1237 the black lines indicate means. Dry and wet seasons are denoted by vertical shading on the
 1238 graph, with the dry season (May to September) highlighted in white and the wet season
 1239 (October to April) in light blue.

Deleted: broken



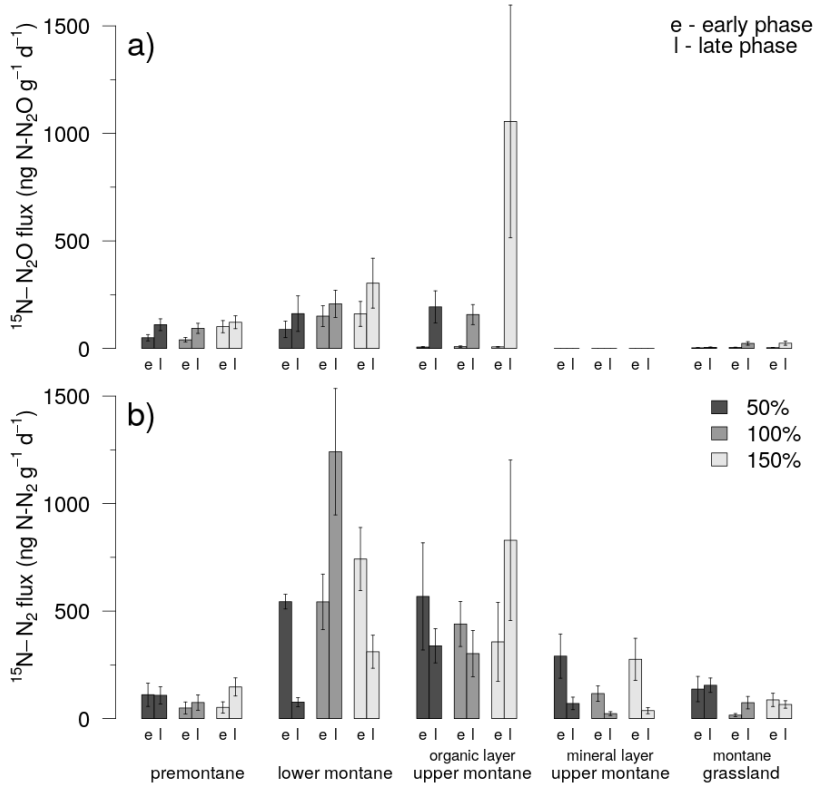
1240
1241

1243 **Figure 4.** Total (a) $^{15}\text{N-N}_2\text{O}$ flux and (b) $^{15}\text{N-N}_2$ flux during the early (≤ 24 hours) and late (> 24
 1244 hours) incubation phases of the water-filled pore space (WFPS) experiment. Results from the
 1245 90 % WFPS treatment are shown in dark-grey, while data from the 70 %, 50 %, and 30 %
 1246 WFPS treatments are shown in mid-grey, light-grey, and white, respectively. The bar charts
 1247 show means and standard errors.



1248
 1249

1250 **Figure 5.** (a) $^{15}\text{N-N}_2\text{O}$ flux and (b) $^{15}\text{N-N}_2$ flux during the early (≤ 24 hours) and late (> 24 hours)
 1251 incubation phases of the NO_3^- addition experiment. Results from the +50 % NO_3^- addition are
 1252 shown in dark-grey, while data from the +100 % and +150 % treatments are shown in mid-
 1253 grey and light-grey, respectively. The bar charts show means and standard errors.



1254